Supporting information

Binding Enhancements of Antibody Functionalized Natural and Synthetic Fibers

Iqra Azeem,[a,b] Marwa El Yaagoubi,[b] Ana M. L. Sousa,[b] Tai-De Li,[c] Basit Yameen,[a]* and King Hang Aaron Lau[b]*

a) Department of Chemistry and Chemical Engineering, Syed Babar Ali School of Science and Engineering (SBASSE), Lahore University of Management Sciences (LUMS), Lahore 54792, Pakistan.
b) Department of Bionanotechnology, University of Strathclyde, Technology and Innovation Centre, 99 George Street, Glasgow G1 1RD, United Kingdom.
c) Advanced Science Research Center (ASRC) of Graduate Center and Department of Physics in City University of New York, CUNY, New York, NY 10031, United States.

Contents

List of Figures

List of Tables

1. Materials

ACS reagent grade Tannic acid (TA), ammonium hydroxide (25% aqueous NH_3), tetraethylorthosilicate (TEOS), enzyme substrate 2,2′-azino-bis(3-ethylbenzothiazoline-6-sulfonic acid) diammonium salt (ABTS), 30% hydrogen peroxide (H_2O_2) were purchased from Sigma-Aldrich (UK) and used without further purification. Polyclonal mouse immunoglobulin G (IgG) produce in goat, horseradish peroxidase (HRP), polyclonal anti-mouse IgG-HRP produce in rabbit (anti-IgG-HRP), and bovine serum albumin (SA) were also purchased from Sigma-Aldrich (UK) and used without further purification. All buffers and sodium chloride (NaCl) were purchased from VWR (UK). Pierce bicinchoninic acid (BCA) protein assay kit was purchased from ThermoFisher. Nanoporous regenerated cellulose (NRC) as filter membranes were purchased from GE Healthcare Life Sciences (GE RC55, 0.45 μm). Cotton and polyester (PE) fabric (100% Polyester Microfiber) were bought from Amazon (UK). The fabrics and NRC were washed with acetone before use. The chemical natures of the substrates were confirmed by ATR-FT-IR.

2. Methods of Nanoparticle Synthesis and Surface Preparation

2.1. Poly(Tannic Acid) (PTA) Coating

Cotton, polyester and NRC sample surfaces were functionalized with the procedure established in our previous publication.[1] Briefly, the samples were washed in acetone and then dipped and gently shaken in a 0.03 mg/mL tannic acid (TA) solution (pH 7.8, 0.1 M Bicine, 0.6 M NaCl) for 1 h. After coating, they were washed three times with DI water, sonicated in the same buffer for 10 minutes, and then washed again with DI water three times to remove any unreacted tannic acid and finally dried with N_2 gas. Coating success was confirmed by silver staining (see Figure S1 in Section 3) for all samples. The chemical natures of the original substrates were characterized by ATR-FT-IR (Figure S2 in Section 4). As examples, PTA coatings on regenerated cellulose and polyester were also characterized by X-ray photoelectron spectroscopy (XPS) (see Section 5).

2.2. "StöberSNP" Surface Modification

Suspended silica nanoparticles (NPs) were first synthesized following the protocol reported by Stöber et al.[2] In brief, a silica nanosol was prepared by adding TEOS (6 mL, 27 mmol) dropwise to a 250 mL 3-neck round bottom flask equipped with a condenser and containing a mixture of ethanol (200 mL) and a 25% aqueous ammonia solution (15 mL, 200 mmol; acting as the base and catalyst). Silica NPs then developed as the nanosol was maintained at 60°C under magnetic stirring at 270 rpm for 5 h. The NPs were separated by centrifugation (12000 rpm, 20 minutes) and washed three times with an ethanol:water

(1:1) mixture. The NP precipitate/pellet was collected and vacuum-dried at 50 °C for 16 h. The NPs were weighed and resuspended in DI water for making suspensions like 0.03, 1, 10, 20 mg. mL^{-1} of such "StöberSNPs" were prepared. Modification experiments to try attach StöberSNPs on cotton fabric samples were performed by immersing 1×1 cm^2 sample pieces into the pre-synthesized StöberSNP suspension for 1 h. Afterwards, the samples were washed with DI water three times to remove excess unbound particles from the surface. The samples were dried at 85°C for 60 min in a vacuum oven prior to use.

2.3. "InSNP" Surface Modification

A combination of Stöber's silica NP synthesis[2] and an *in situ* modification protocol reported by Manatunga et al.[3] were modified for *in situ* growth of silica NP on the sample surfaces. A silica nanosol slightly modified from the StöberSNP method was again prepared, but the samples were immersed in it at an earlier stage before "large" solution-phase silica NPs could develop. Specifically, for the nanosol, 5.0 mL of 25% aq. NH_4OH was added dropwise into ethanol (100 mL) while stirring at 50ºC in 30–45 min. Then TEOS (6.0 ml) was added to the ethanol-ammonia mixture in a dropwise manner under vigorous stirring at the same temperature (the slow addition is critical to obtain uniformity in NP size). After 1 h, 1×1 cm^2 sample pieces were immersed in the prepared silica nanosol and stirred overnight at 50ºC. Afterward, the samples were washed with DI water three times to remove excess unbound silica. The samples were then dried at 85°C for 30 min in a vacuum oven prior to use.

2.4. Protein Immobilization

Both IgG immobilization and SA-IgG co-immobilization used the same basic protocol. Proteins were prepared in pH 7.4 PBS at the concentrations specified in the main text. The SA standard of the BCA assay kit was used for immobilization experiments, so its original concentration is known from the supplier (2 mg/mL), and solutions were diluted accordingly for experiments. IgG solutions were prepared at the specified concentrations by appropriate dilutions directly from the entire aliquot bought from the supplier (0.5 mL at 1 mg/mL). The protein solutions were filtered slowly with a 0.2 μm hydrophilic syringe filter (PES or cellulose acetate) before use to remove bubbles and to sterilize the solutions. Protein concentrations were determined following a commercially available QuantiPro" BCA protein assay protocol (see Figure S5). Solutions with low protein concentrations were prepared from serial dilution of samples at a higher concentration falling within the range of the BCA assay. All substrates (types I-VI as specified in Figure 1 of the main text) were immersed in protein solutions for 1 h with constant stirring with an orbital shaker and then rinsed with PBS. Around 1 mL of solution was used for each 1x1 cm^2 sample piece.

2.5. Immobilized IgG Surface Activity Assay

Samples functionalized with the mouse IgG, with or without SA co-immobilization, were first incubated for 1 h in a solution of 1 mg/mL SA (Sigma, lyophilized powder) from as a blocking agent against non-specific protein adsorption/binding, as is standard practice in many immunoassay protocols. Then the samples were incubated for 1 h in a 10 μg/mL solution of HRP-conjugated anti-IgG (anti-IgG-HRP) in pH 7.4 PBS. The concentration of anti-IgG-HRP was confirmed using the BCA assay (Figure S5).

An HRP enzyme assay was then performed on samples held to the sides of standard 5 mL UV cuvettes using custom-built holders, as established previously.[1] Briefly, a mixture of 1.9 mL of 9.1 mM ABTS in PBS, 70 μL of 0.3% v/v H_2O_2, and 35 μL of pH 7.4 PBS was added to the UV cuvette (the last 35 μL PBS was added to make up the total volume to 2 mL; in a regular assay of enzymes dissolved in solution, this would be the enzyme sample). The absorbance of the oxidized ABTS accumulated in solution, catalyzed by the surface bound anti Mouse-IgG-HRP, was measured every 2 minutes for 20 minutes at 405 nm wavelength with a UV-vis absorption spectrometer (Jasco V-660). Between each time point, the assay solution was stirred using a mini magnetic bar placed inside the cuvette. The activity was then calculated from the known molar extinction coefficient of oxidized ABTS and the slope of absorbance vs. time for the portion of the curve that showed a steady-state linear increase. Our HRP assay and the equivalent amount of surface bound IgG-HRP was also verified by a regular assay of different amounts of HRP dissolved in solution (Figure S6).

3. Silver Staining of PTA Coated Fabric

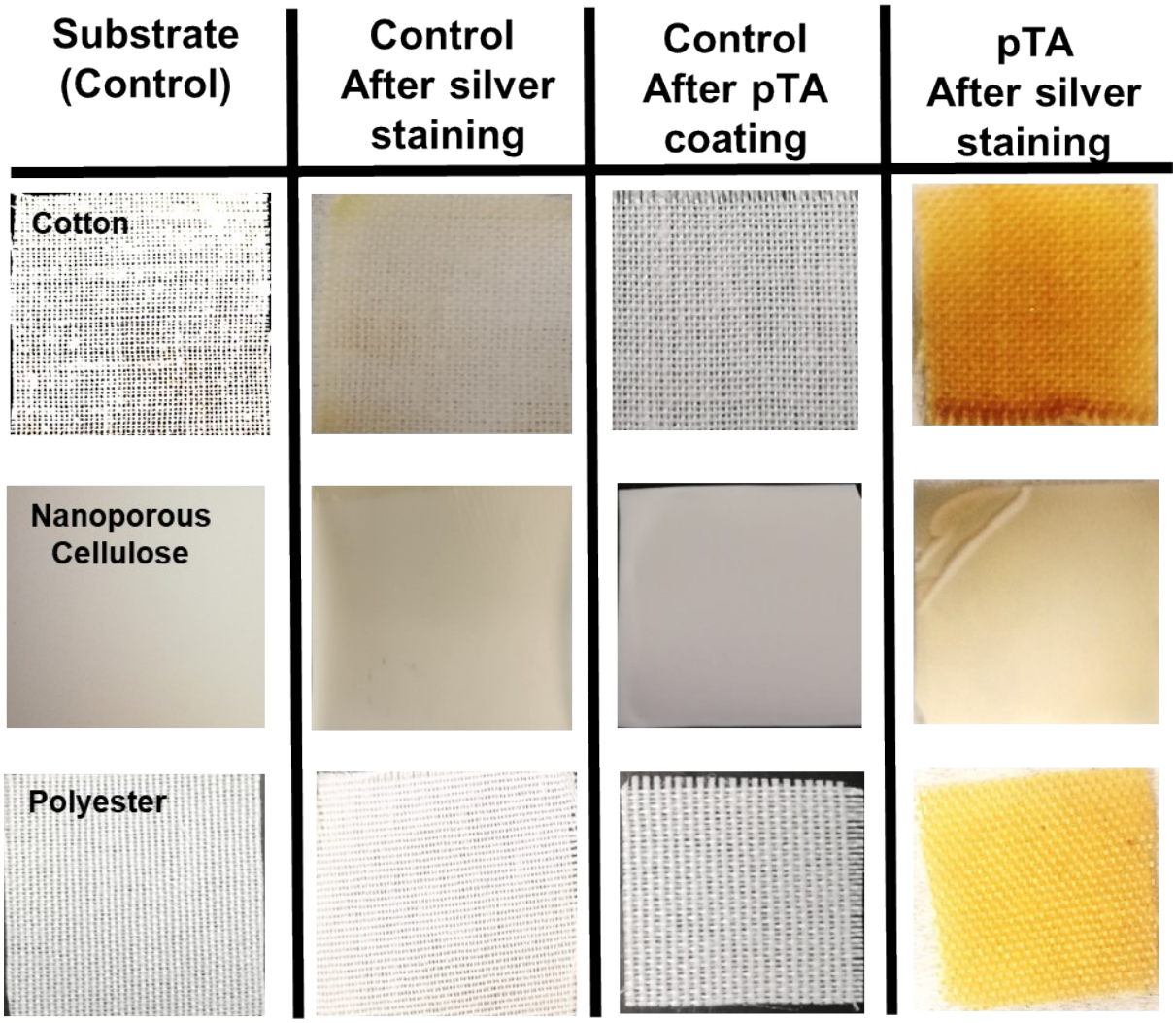

Figure S1. Silver staining of substrate performed by incubating the sample in 25mM AgNO3 for 1h, the OH group of tannic acid reduced silver ions that resulted in deep coloration.

4. FT-IR Characterization of Native Cotton, NRC and Polyester

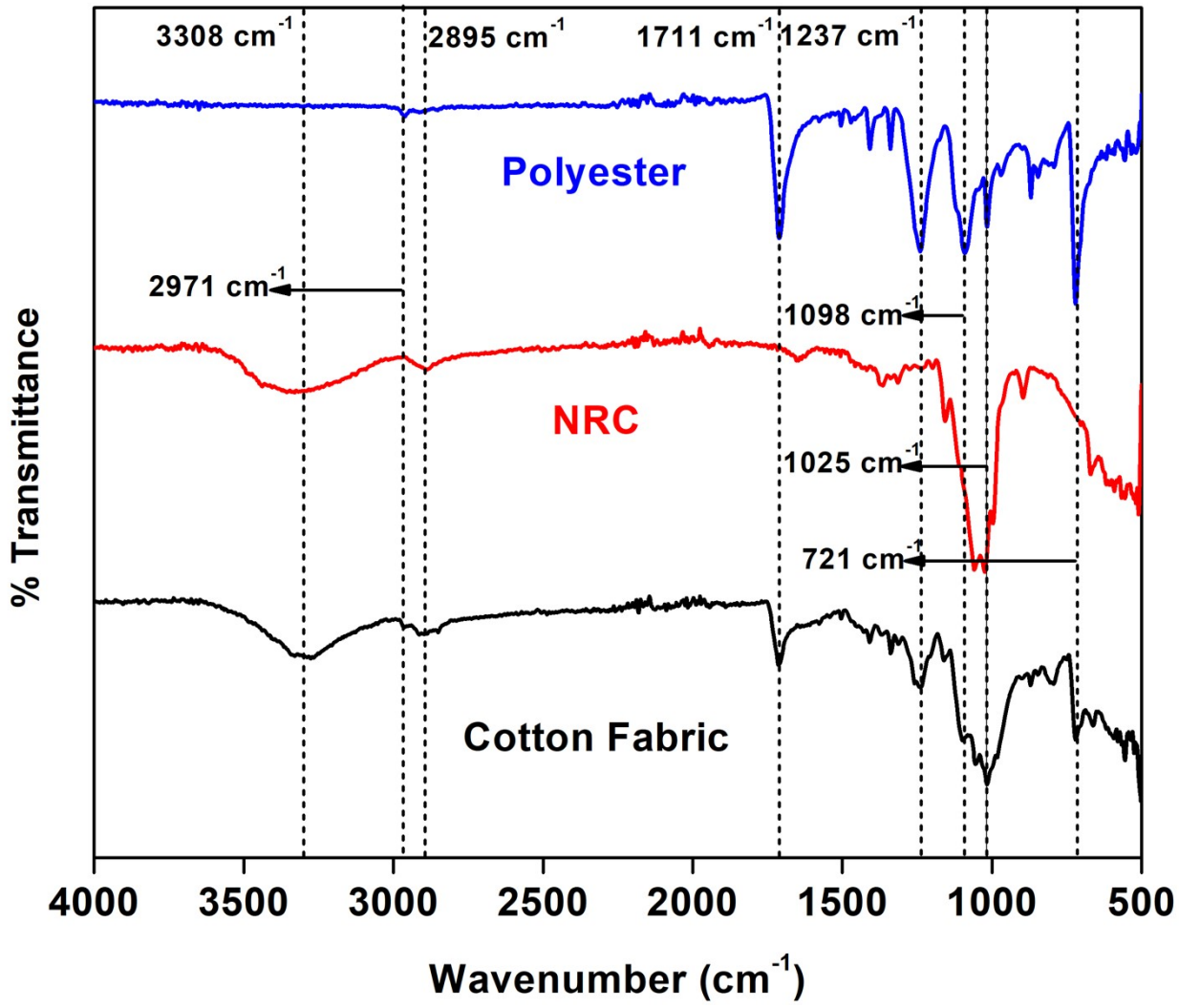

Figure S2. FT-IR spectrum of native (a) cotton, (b) nanoporous regenerated cellulose (NRC), and (c) polyester (PE) fabric.

ATR-FT-IR showed bands consistent with both the substrates and PTA. Figure S2 shows the spectra for the native substrates before functionalization. For polyester, the characteristic alkyl C-H stretch at 2971 cm^{-1}, C-H bending at 1237 cm^{-1}, strong peak of carbonyl group (C=O) asymmetric stretch at 1711 cm^{-1} and aromatic sp^2 C-H bending at 721 cm^{-1} were observed. The spectra of native cotton and NRC showed the same characteristic bands of cellulose: OH asymmetric stretching bands around 3308 cm^{-1}, aliphatic alkyl (CH_2 and CH) asymmetric stretching at 2895 cm^{-1}, and ether linkage (C-O) asymmetric stretch at 1098 cm^{-1} and 1025 cm^{-1}. The cotton fabric sample also showed some of the bands for polyester (e.g. 1711 cm^{-1}, 1237 cm^{-1}, 721 cm^{-1}) and could indicate some fabric blending.

Characterization after PTA coating was not particularly revealing because PTA has overlapping chemical groups with both substrates (e.g. OH, C-O ether linkage, C=O carbonyls, aromatic sp^2 C-H) and our very thin coatings (see ESI Section 0) contribute very little IR absorption compared to the signal from the bulk of the substrate fibers. Indeed, IR measurements showed very similar spectra (not shown).

5. X-Ray Photoelectron Spectroscopy (XPS) Characterization of PTA

Nanoporous regenerated cellulose (NRC) and polyester (PE) samples were analysed by XPS (VersaProbe II from Physical Electronics). Cotton samples also have the same cellulosic nature as NRC and at most have some PE blending (see FT-IR spectrum in Section 4). Since there was a limitation to XPS instrument access, we used the NRC samples as a proxy for the properties of cotton. All XPS measurements were done with Al Kα X-rays, 45° take-off angle, under low energy electron and Ar+ surface charge compensation, with 23.5 eV pass energy for high resolution and 117.4 eV for survey spectra. The binding energy of the main C1s peak at 284.8 eV (C-C/C-H) was used to correct for specimen charging. C1s and O1s fitting assumed Gaussian peak components and equal peak widths (except for C1s π–π* shake-up).

Table S1. Atomic percentages measured from XPS survey scans for carbon (%C) and oxygen (%O) on PE samples, with and without PTA coating. The C1s and O1s integrated peak areas, the corresponding sensitivity factors used for calculation,* and the "ideal" percentages present according to the chemical structures of PE and PTA, are also shown. See Figure 1a in the main text for the assumed chemical structures.

	%C	%O		C1s measured peak area	O1s measured peak area	C1s sensitivity factor (SC1s)	O1s sensitivity factor (SO1s)
PE control	71%	29%		35,842	34,378	0.314	0.733
Ideal (PE)	71%	29%		n/a	n/a	n/a	n/a
PTA on PE	69%	31%		31,333	33,150	"	"
Ideal (PTA)	62%	38%		n/a	n/a	n/a	n/a

5.1. Atomic composition analysis of polyester (PE) samples before and after PTA coating

XPS survey scans show that the carbon and oxygen atomic percentages (%C and %O respectively) for both NRC and PE samples changed after PTA coating in the directions expected from the differences in chemical structures between PTA and the substrates. The data for PE is shown in Table S1. Before coating, %C and %O (71% to 29%) are consistent with the chemical structure of poly(ethylene

* The atomic percentages are calculated as: $atomic\,\% = \frac{n_i/S_i}{\sum\left(n_i/S_i\right)}$, where n_i is the integrated area of species i.

terephthalate) (PET) (Figure 1 in the main text), a common material used for polyester fabrics. In contrast, the atomic percentages of PTA are 62 %C to 38 %O (76 carbons and 46 oxygens per molecule of TA). Correspondingly, %C and %O (slightly) decreased and increased, respectively, to 69 %C and 31%O for the PTA coated PE sample. Although these changes are small, they are corroborated by the chemical shifts of high resolution C1s chemical shifts (Figure S3).

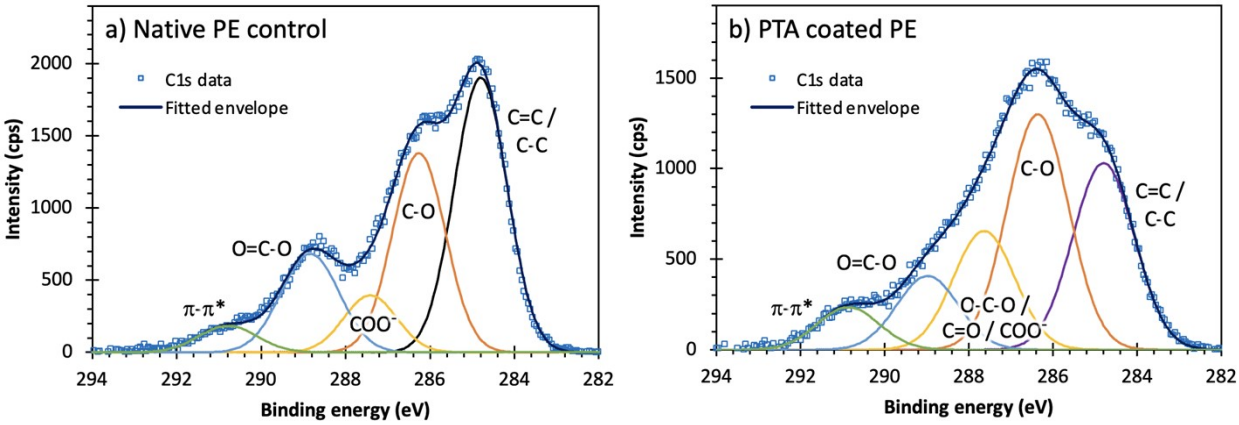

Figure S3. High resolution XPS C1s spectra for (a) native and (b) PTA-coated polyester (PE) samples. The deconvoluted peaks are labeled with their chemical shift assignments. The relative peak areas are listed in Table S2.

Table S2. Relative peak areas of the deconvoluted chemical shifted C1s peaks for polyester samples shown in Figure S3, listed together with the "ideal" percentages corresponding to the chemical structures of PET monomers and a TA molecule. The fitted binding energies corresponding to each peak (averaged between data for the native and PTA coated samples) are also listed.

	C-C / C=C (284.8 eV)	C-O (286.3 eV)	COO^- / C=O / O-C-O (287.5 eV)	O=C-O (288.9 eV)
PE control	43%	31%	9%	17%
Ideal (PE)	60%	20%	0%	20%
PTA on PE	30%	38%	19%	12%
Ideal (PTA)	39%	46%	1%	13%

5.2. C1s chemical shifts of PE samples before and after PTA coating

According to the monomer structure of PET, this polyester should have a 60:20:20 % ratio of aromatic (C=C) to ether (C-O) to ester carbons (O=C-O) (Table S2). In comparison, the chemical structure of tannic acid gives a 39:46:13 % ratio of aromatic/aliphatic (C-C) to ether/hydroxyphenyl (C-O) to ester carbons (O=C-O). Although we did not exactly observe the corresponding C1s chemical shift peak ratios

in our unmodified polyester sample (Figure S3a), we did observe the expected reversal in relative ratios of C-C/C-O carbons, i.e. a prominent C-O peak significantly higher in intensity than the C-C peak was observed in the PTA-coated sample (Figure S3b). There was also a higher O-C-O/C=O peak around 287.5 eV, which can be attributed to quinones (C=O) and crosslinking adducts of the PTA coating. The higher π–π* shake up peak compared with the native polyester would also be consistent with the larger amounts of galloyl groups (i.e. trihydroxybenzoates) comprising the bulk of the polyphenol coating. Thus overall, the presence of various anticipated changes in the C1s high resolution spectra shown in Figure S3 clearly indicates that PTA coating on polyester was successful.

Nonetheless, our data deviate from the "ideal" C1s peak ratios of the PET monomer in having a stronger C-O peak and in the appearance of a peak around 287.5 eV, which we assign to hydroxyls and acid carbons (COO^-), respectively. These features could be contributed from dissociation of ester linkages, perhaps as a result of the application of fabric softeners, which are caustic agents, on the samples during fabric manufacturing-processing. Some sample damage from the electron and Ar+ charge compensation beams might also have dissociated the aromatic terephthalate groups of PET, reducing the intensity of the C=C peak and producing additional carbon-oxygen groups that contributed to the intensities of C1s peaks with energies higher than the C=C carbons.

Table S3. Atomic percentages calculated from XPS survey scan data for carbon (%C) and oxygen (%O) on nanoporous regenerated cellulose (NRC) samples, with and without PTA coating. The respective C1s and O1s integrated peak areas, the corresponding sensitivity factors used for calculation,* and the "ideal" atomic percentages present according to the chemical structures of PE and PTA ("ideal"), are also shown. See Figure 1 in the main text for the assumed chemical structures.

	%C	%O		C1s measured peak area	O1s measured peak area	C1s sensitivity factor (S_{C1s})	O1s sensitivity factor (S_{O1s})
NRC control	53%	47%		45,221	93,838	0.314	0.733
Ideal (cellulose)	50%	50%		n/a	n/a	n/a	n/a
PTA on NRC	57%	43%		58,077	101,962	"	"
Ideal (PTA)	62%	38%		n/a	n/a	n/a	n/a

5.3. Atomic composition analysis of NRC samples before and after PTA coating

Regarding results for the NRC samples, the %C and %O data measured from survey scans (Table S3) again show atomic ratios and changes consistent with the chemical structure of NRC (i.e. cellulose) and

the presence of the PTA layer after coating. Cellulose has equimolar C and O and the ratio measured for the native NRC sample was quite close at 53%C to 47%O. A small amount of adventitious carbon is to be expected. After PTA coating, the C:O ratio increased to 57%:43%, consistent with the higher number of carbons per molecule of TA (76 carbons to 46 oxygens). These changes are also corroborated by the chemical shifts of high resolution C1s chemical shifts (Figure S4).

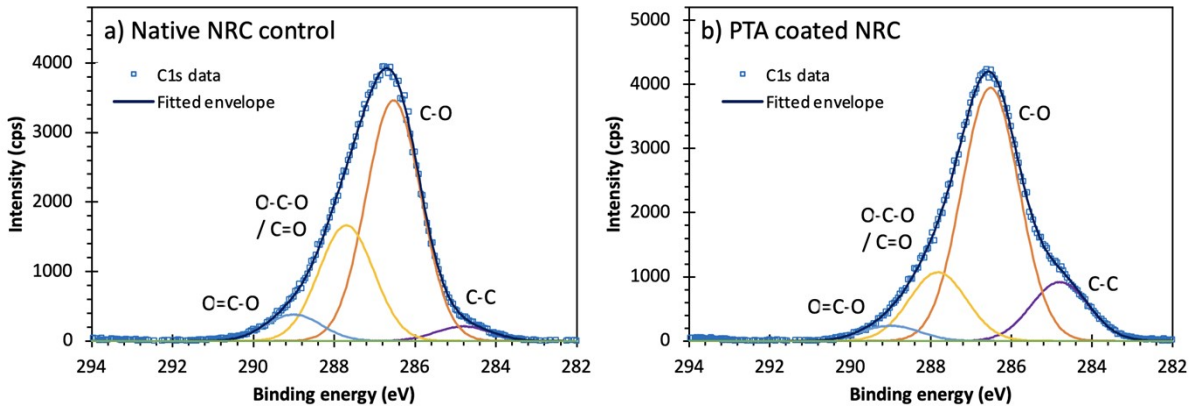

Figure S4. High resolution XPS C1s spectra for (a) native and (b) PTA-coated nanoporous regenerated cellulose (NRC) samples. The deconvoluted peaks are labeled with their chemical shift assignments. The relative peak areas are listed in Table S4.

5.5. C1s chemical shifts of NRC samples before and after PTA coating

According to the monomer structure of cellulose, there should be a ratio of 83% to 17% hydroxy/ether (C-O) to diether carbons (O-C-O), and no aliphatic carbons (C-C) nor esters/acids (Table S4). In contrast, as already discussed above, TA has many aromatic and aliphatic carbons (C-C/C=O) and almost as many hydroxyphenyls (C-O). Accordingly, Figure S4 shows a significant increase in the C-C/C=C peak intensity after PTA coating (15% vs 2% amongst C1s species—Table S4). The C-O peak was still highly prominent, since hydroxyl carbons are present in both cellulose and PTA, but the relative percentage of C-O was lower (65%, decreased from 71%). However, similar to the polyester samples, we observed a relative decrease in the O=C-O peak, although TA has a number of benzoate esters. The native NRC sample also appeared to show a C-O:O-C-O ratio (71% :22%) lower than indicated by the chemical structure of cellulose (83% :17%). Nonetheless, the intensity of the O-C-O peak did drop after PTA coating (down to 17%), consistent with a thin coating of PTA on the NRC, since PTA is not supposed to have O-C-O bonds. Thus, overall, the changes in the C1s chemical shift data after PTA coating shown in Figure S4 and Table S4 clearly indicates that PTA coating on NRC was also successful.

Table S4. Relative peak areas of the deconvoluted chemical shifted C1s peaks for NRC samples shown in Figure S4, listed together with the "ideal" percentages corresponding to the chemical structures of cellulose monomers and a TA molecule. The fitted binding energies corresponding to each peak (averaged between data for the native and PTA coated samples) are also listed.

	C=C / C-C (284.8 eV)	C-O (286.6 eV)	COO- / C=O / O-C-O (287.9 eV)	O=C-O / COOH (289.2 eV)
NRC control	2%	71%	22%	4%
Ideal (cellulose)	0%	83%	17%	0%
PTA on NRC	15%	65%	17%	3%
Ideal (PTA)	39%	46%	1%	13%

5.6. PTA Coating Thickness Estimation

PTA thickness determination on the microfiber samples is difficult because traditional measurement techniques (e.g. ellipsometry, profilometry, QCM, etc.) are only suited to characterization of thin films on flat substrates. XPS thickness calculation requires peak data that exclusively indicate either the substrate or coating but our PTA, cellulosic and polyester materials share similar chemical groups and hence XPS peaks. One possibility is to pick one of the C1s chemical shifts with the least contribution from the substrate for calculation and assume that the necessary reference for the intensity of pure PTA (I^{∞}) corresponds to the composition, i.e. relative peak area (A_{ideal}) of ideal PTA (see e.g. Table S4). Then the conventionally required peak intensity to indicate the film/coating (I_{coating}) can be equated to the measured relative area of the chosen characteristic C1s peak (A_{coating}), and related to the thickness (d) by the commonly used equation:[4]

$$\frac{I_{coating}}{I^{\infty}} = \frac{A_{coating}}{A_{ideal}} \propto 1 - e^{-d/\lambda}$$

where λ is the effective attenuation length, i.e., λ = 2.9 nm for C1s photoelectrons with kinetic energy around 1200 eV,[4] corresponding to the difference of Al Kα (1486.6 eV) and C1s binding energies (285 eV).

On NRC, there should ideally be no peak for the C-C chemical shift in the cellulose substrate, except for the fact that there is always some contribution from adventitious carbon contamination. Assuming that the entire 15% C-C composition after PTA deposition (Table S4) is entirely due to the polyphenol coating

and ratioing this to the ideal 39% C-C composition of tannic acid, a PTA thickness on NRC (and by extension, on cotton) is calculated to be 1.4 nm.

On polyester, as discussed in Section 0, there is some ambiguity in the interpretation of the higher than expected ~287.9 eV chemical shift intensity, which corresponds to the overlapping COO^- and C=O contributions that can be assigned to, respectively, dissociated ester bonds in native polyester and quinone formed from PTA oxidation (similar excess C=O intensity also observed for PTA coated NRC). With these "excess" COO^-/C=O intensities, the measured relative areas of the C-C and C-O chemical shifts (Table S2) were lower than expected. For example, for the purpose of comparing with the ideal PTA composition, some of the ~287.9 eV intensity potentially arising from PTA quinone C=O should be counted towards PTA hydroxyphenyl C-O at ~286.3 eV, from which it is derived. On the other hand, the actual underlying polyester substrate might still be contributing some of the C-O intensity to the measurement after PTA coating. Assuming that only the 7% increase in C-O area (Table S2) is attributed to PTA, and using the ideal PTA C-O composition of 46% as reference, the thickness is calculated to be 0.5 nm. If instead the entire 38% C-O area measured after coating is taken at face value and attributed to PTA, a thickness of 5 nm is obtained. If it is further assumed that the 10% difference in the ~287.9 eV intensity is attributed to quinone C=O and added to the 38% C-O area measured (Table S2), then the relative area becomes similar to the PTA ideal. This potentially matches the fact that the measured 12% relative area measured for O=C-O at ~288.9 eV is also close to the 13% ideal for pure PTA. However, there is always some uncertainty in XPS measurements and also its peak fitting. Assuming that the coating signal just matches the pure material reference, the thickness is ~13 nm at 99% attenuation (given $\lambda = 2.9$ nm; the equation is undefined at 100% attenuation). Overall, the estimated range of thickness from 0.5 to 13 nm on polyester includes a number of uncertainties. We had previously estimated a narrower range of 2 to 6 nm for PTA coatings on alumina prepared variously from pH 7 to 8.5, similar to the currently used conditions.[1] It may be that taking the measured 38% C-O area at face value, giving a 5 nm thickness, is the simplest interpretation for the polyester sample.

6. BSA Calibration Curve to Measure the Amount of Unknown Protein Concentration

In order to determine the concentration of the IgG, SA and HRP samples for immobilization studies, a BCA assay (Pierce BCA Protein Assay Kit from ThermoFisher) was applied to a set of solutions for each protein spanning a range of concentrations prepared in PBS by serial dilution. The results were then compared to a standard curve obtained from measurements of a bovine serum albumin (BSA) calibration sample with a known concentration provided in the kit. For each measurement, briefly, to 100 µL of each sample, 2.0 mL of working reagent, prepared by mixing 50parts of reagent A and 1 part of reagent B from the assay kit, was added in a glass vial. The vial was covered and incubated at 37ºC for 30 min. The vial was then cooled down to room temperature. Afterward, absorbance at 562 nm was measured with a UV-vis absorption spectrometer (Jasco V-660) for all the samples within 10 minutes.

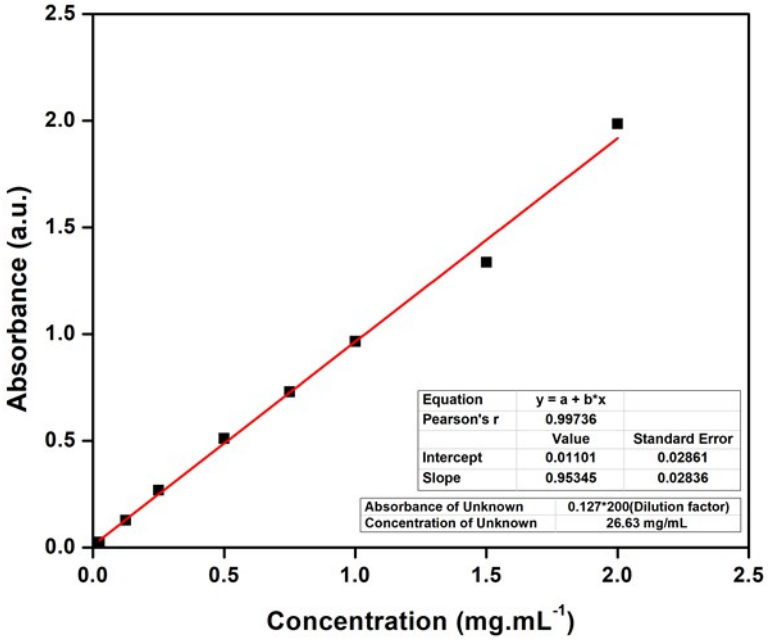

Figure S5. BCA assay absorbance over a range of BSA calibrant concentration.

7. Enzyme Assay to Determine HRP Concentration

A common peroxidase activity assay using ABTS as the enzyme substrate was carried out to obtain a standard curve for solutions of HRP over a range of concentrations from 3.9 µg/mL to 375 µg/mL (see Figure S4 and Table S1 below). For each HRP sample in solution, 1.93 mL of 9.1 mM ABTS, 70 µL of 0.3 % v/v H_2O_2, and 35 µL of HRP solution in pH 7.4 PBS were mixed together in a 5 mL UV cuvette. The HRP concentrations were previously determined using the BCA protein assay (see Section 6 and Figure S5). The absorbance of the oxidized ABTS was then measured at 405 nm every 2 min for 20 min with a UV-vis absorption spectrometer (Jasco V-660). Between each time point, the assay solution was stirred using a mini magnetic bar placed inside the cuvette. The activity was then calculated from the known molar extinction coefficient of oxidized ABTS and the slope of absorbance vs. time for the portion of the curve that showed a steady-state linear increase. The results of this set of solution-phase standard measurements are shown in Table S5 and Figure S6 below.

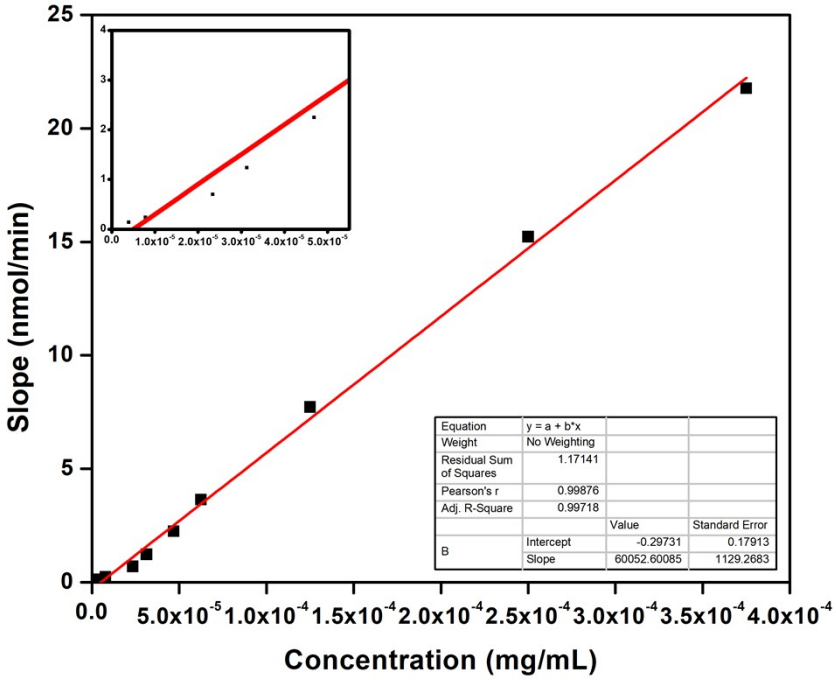

Figure S6. HRP activity in an ABTS enzyme assay at a range of enzyme concentrations. The concentration range chosen is comparable to the equivalent amounts of surface bound HRP-conjugated IgG on our fabric samples (see Section 17).

Table S5. Values calculated to plot the standard calibration curve between the concentration of HRP (mg/mL) and Slope (mol/min).

Sr.No.	X-axis = Conc. of HRP (mg/mL)	Slope (min^{-1}) measured from time-course experiment	Slope in mol/L/min = S = [Slope (min^{-1})/molar absorptivity (Ɛ)]*path length (l) = Ɛ = 36800 mol/L/cm l = 1cm	Y-axis = Slope (mol/min) = S* 0.00201 L
1.	0.000375	0.3985	1.08E-05	2.18E-08
2.	0.00025	0.3985	7.57E-06	1.52E-08
3.	0.000125	0.3985	3.84E-06	7.72E-09
4.	6.25E-05	0.3985	1.82E-06	3.65E-09
5.	4.69E-05	0.3985	1.12E-06	2.25E-09
6.	3.13E-05	0.3985	6.14E-07	1.23E-09
7.	2.34E-05	0.3985	3.48E-07	6.99E-10
8.	7.8E-06	0.3985	1.2E-07	2.4E-10
9.	3.9E-06	0.3985	6.79E-08	1.37E-10

8. E-SEM Surface Characterization

Field-Emission Environmental Scanning Electron Microscope (FEI Quanta 250) was used to image the microstructured fabric sample after StöberSNPs and inSNPs immobilization at low pressure of 1 mbar and at low 5kV acceleration voltage to reduce surface charging.

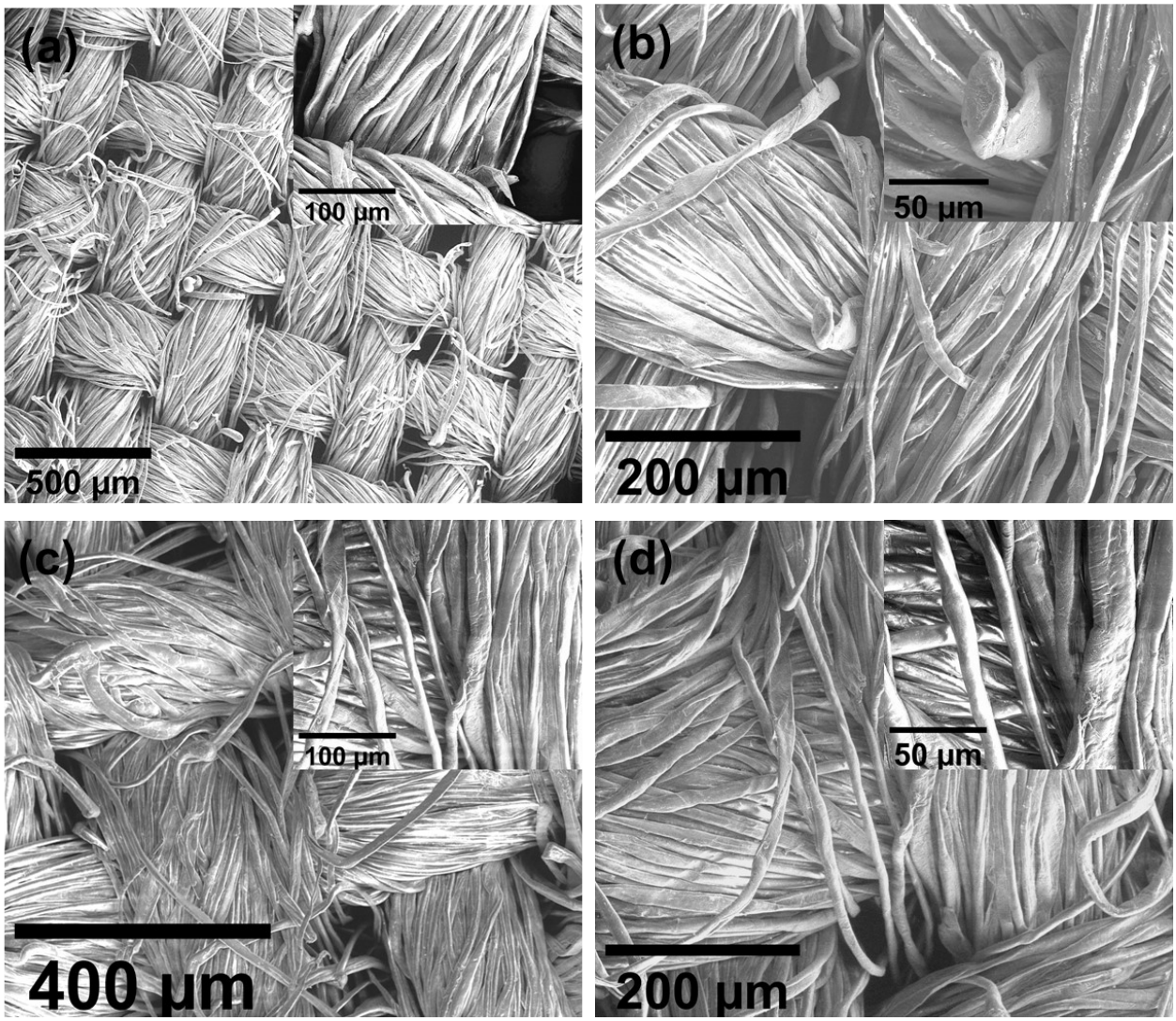

Figure S7. Typical ESEM images of (a) & (b) native and (c) & (d) PTA-coated cotton fabric. Insets show higher resolution images of the corresponding samples.

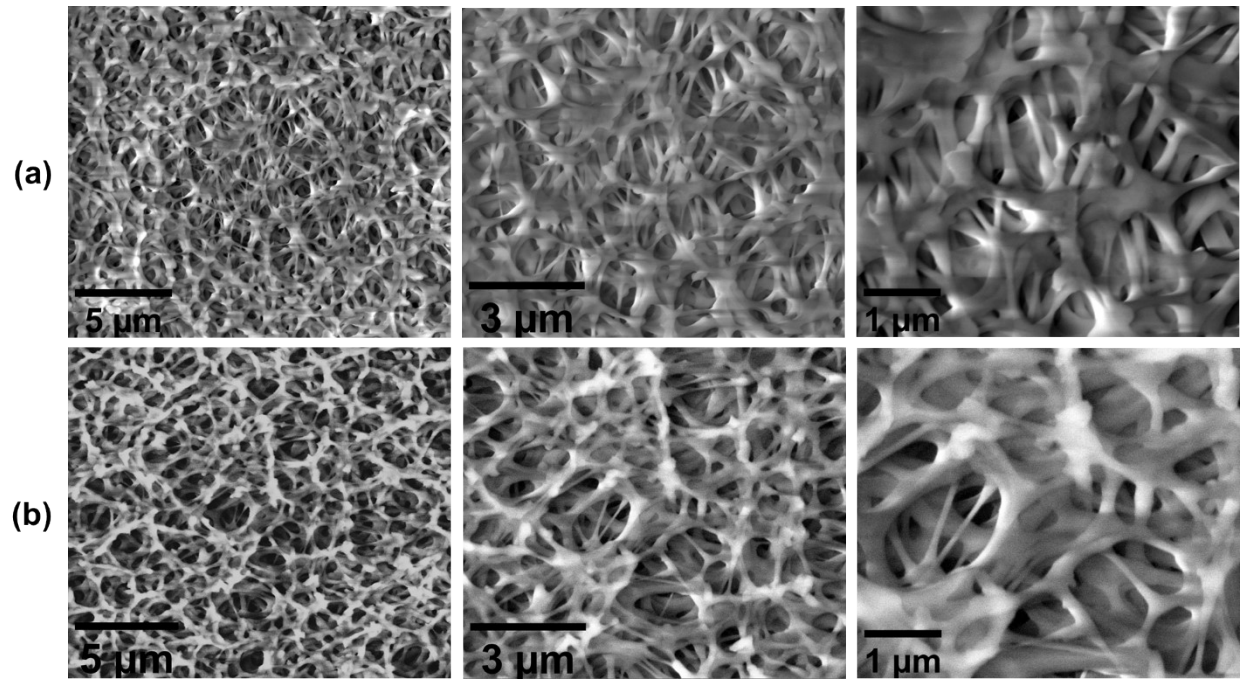

Figure S8. Typical ESEM images of (a) native (b) PTA-coated nanoporous regenerated cellulose (NRC) paper.

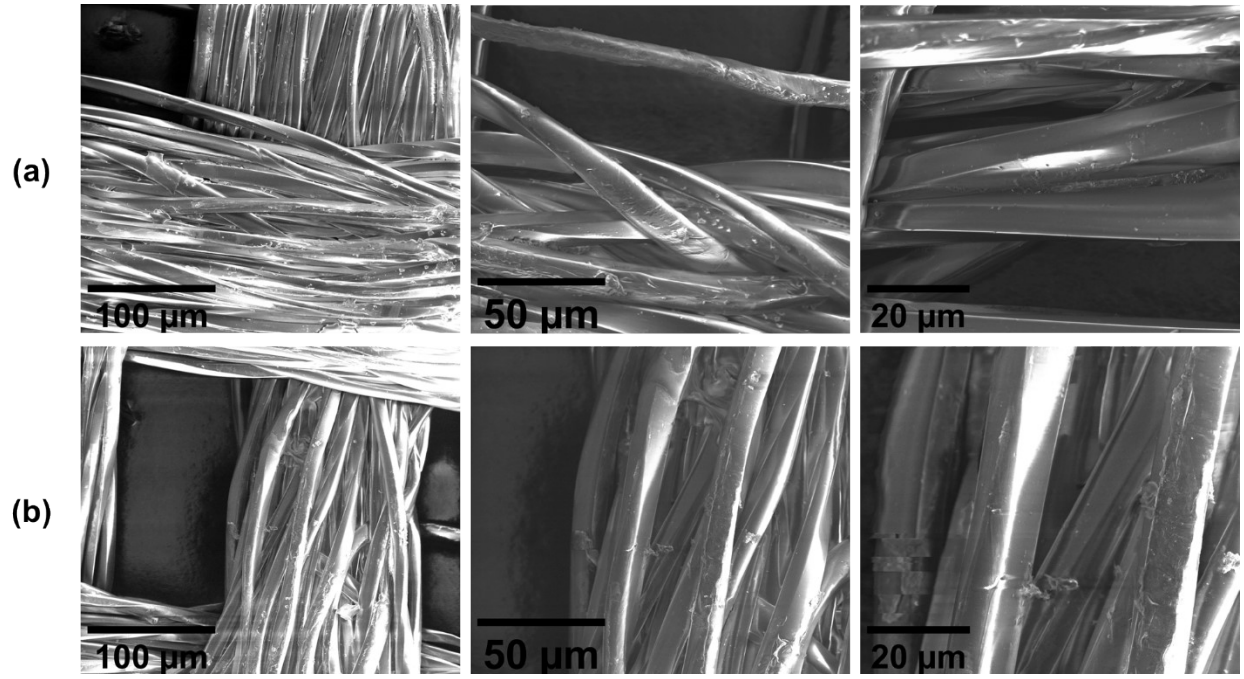

Figure S9. Typical ESEM images of (a) native (b) PTA-coated polyester (PE) fabric.

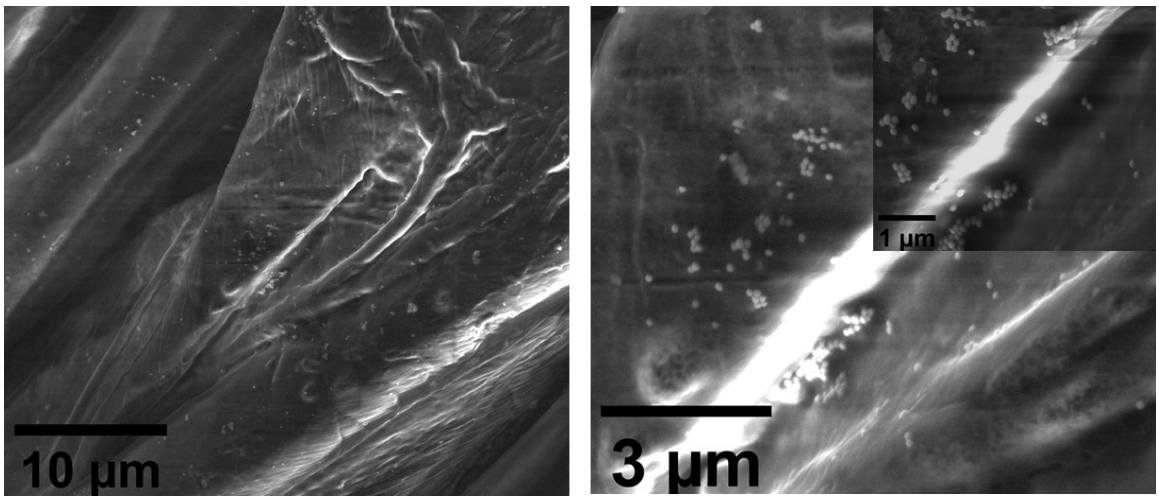

Figure S10. E-SEM images of 10 mgmL-1 aqueous suspensions of StöberSNPs on PTA coated cotton fabric. Inset shows the SEM image at higher resolution.

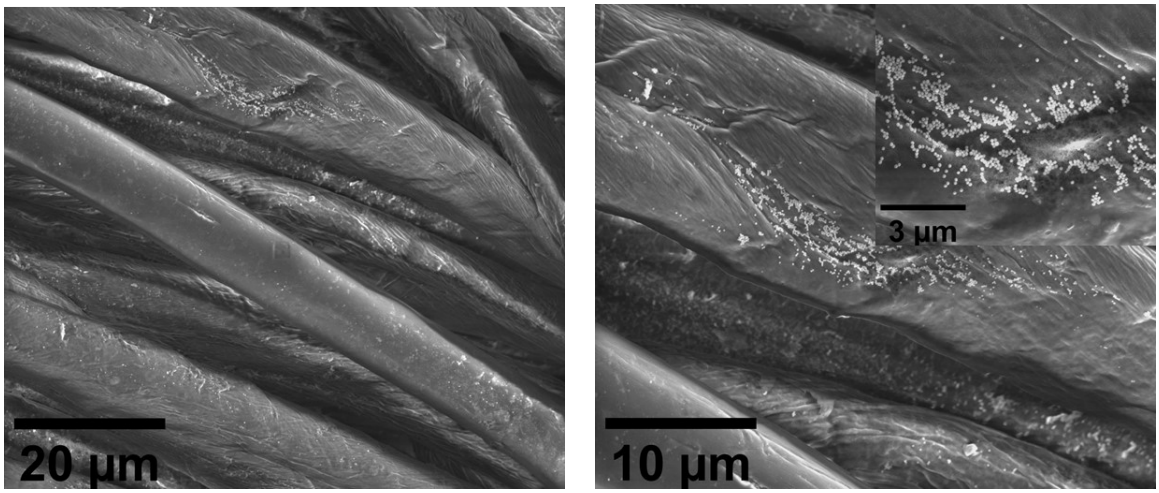

Figure S11. E-SEM images of 20 mgmL-1 aqueous suspensions of StöberSNPs on PTA coated cotton fabric.

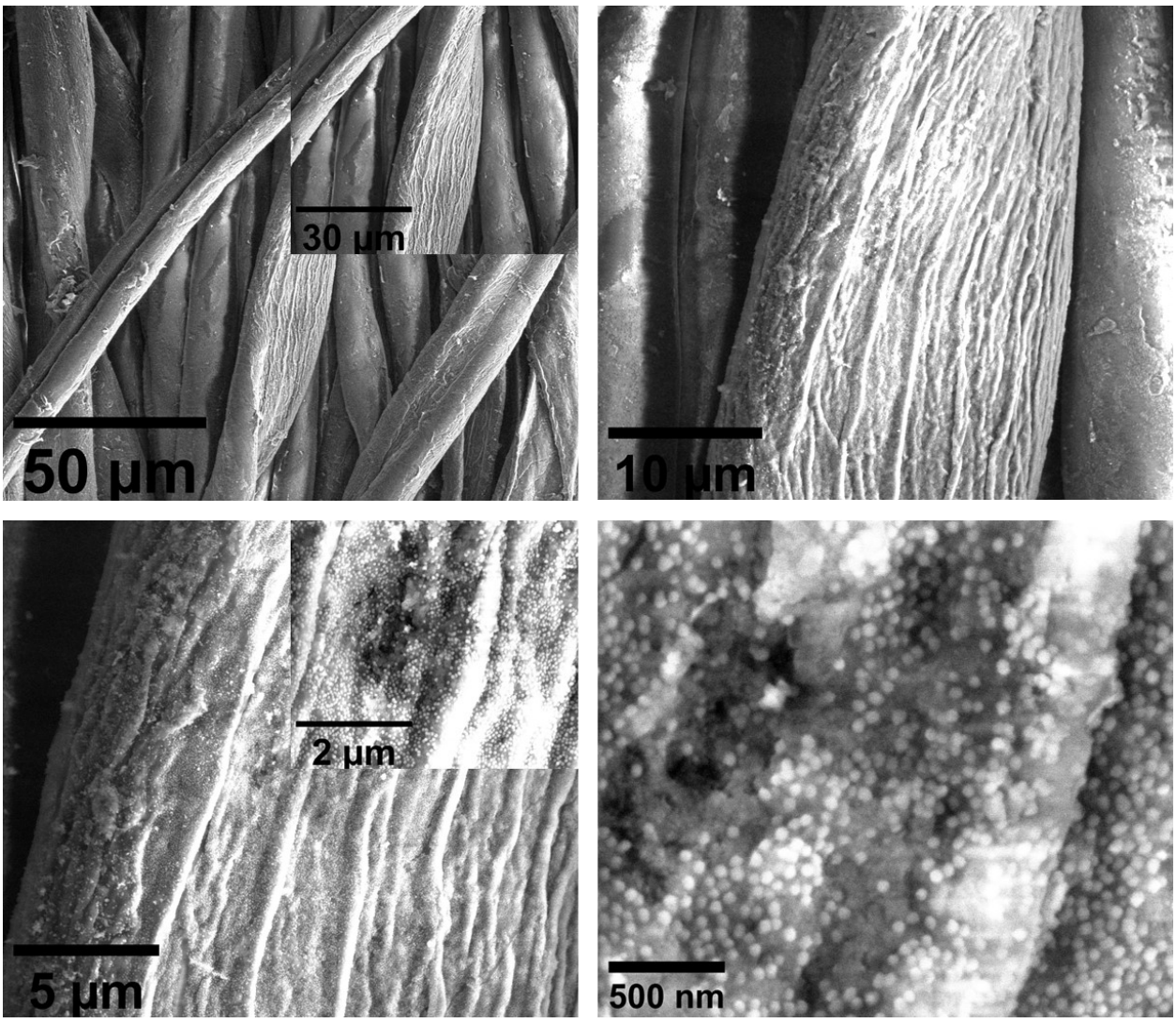

Figure S12. E-SEM images of inSNPs on native cotton fabric. Insets show higher magnification images of the corresponding samples.

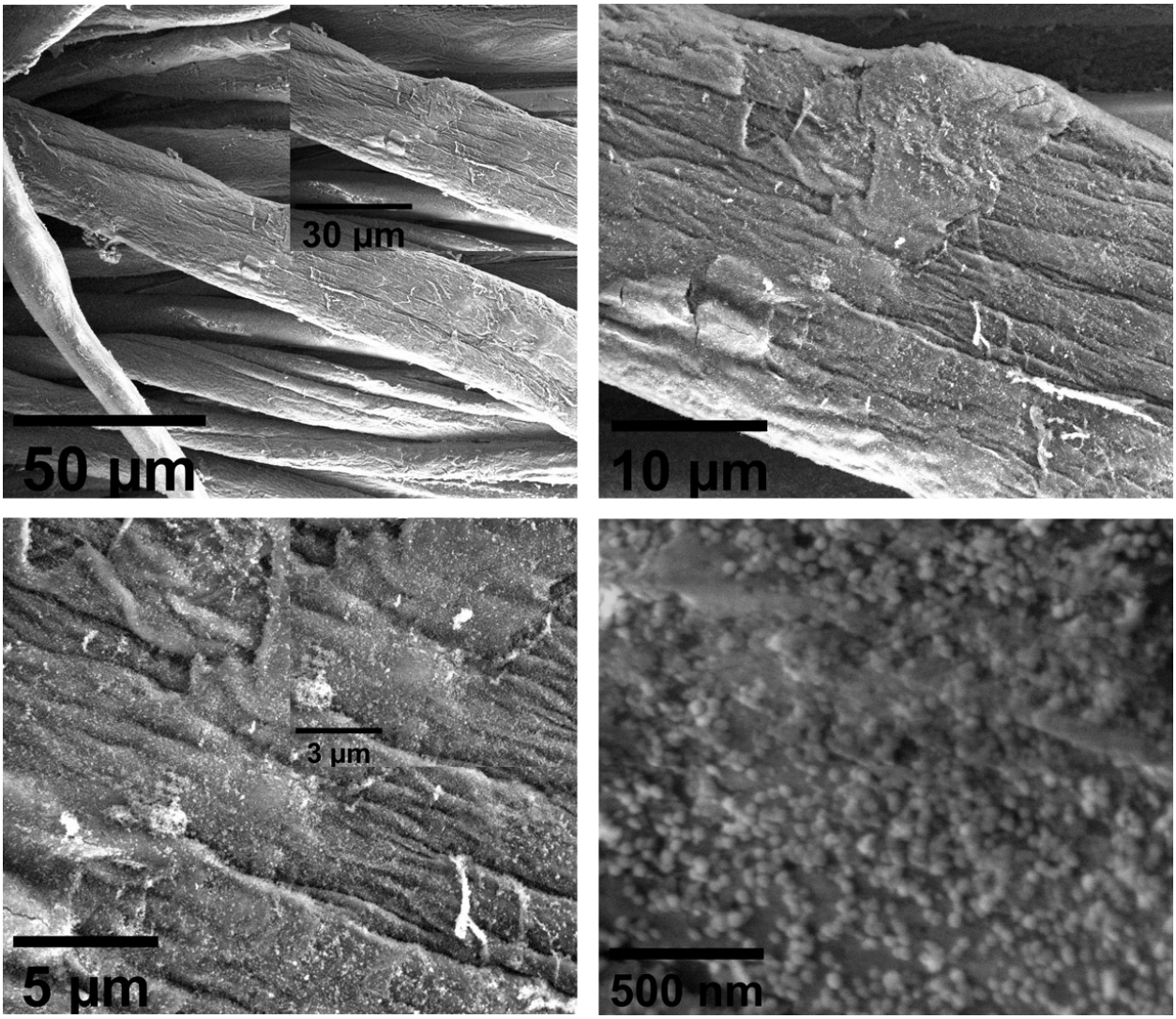

Figure S13. E-SEM images of inSNPs on PTA coated cotton fabric.

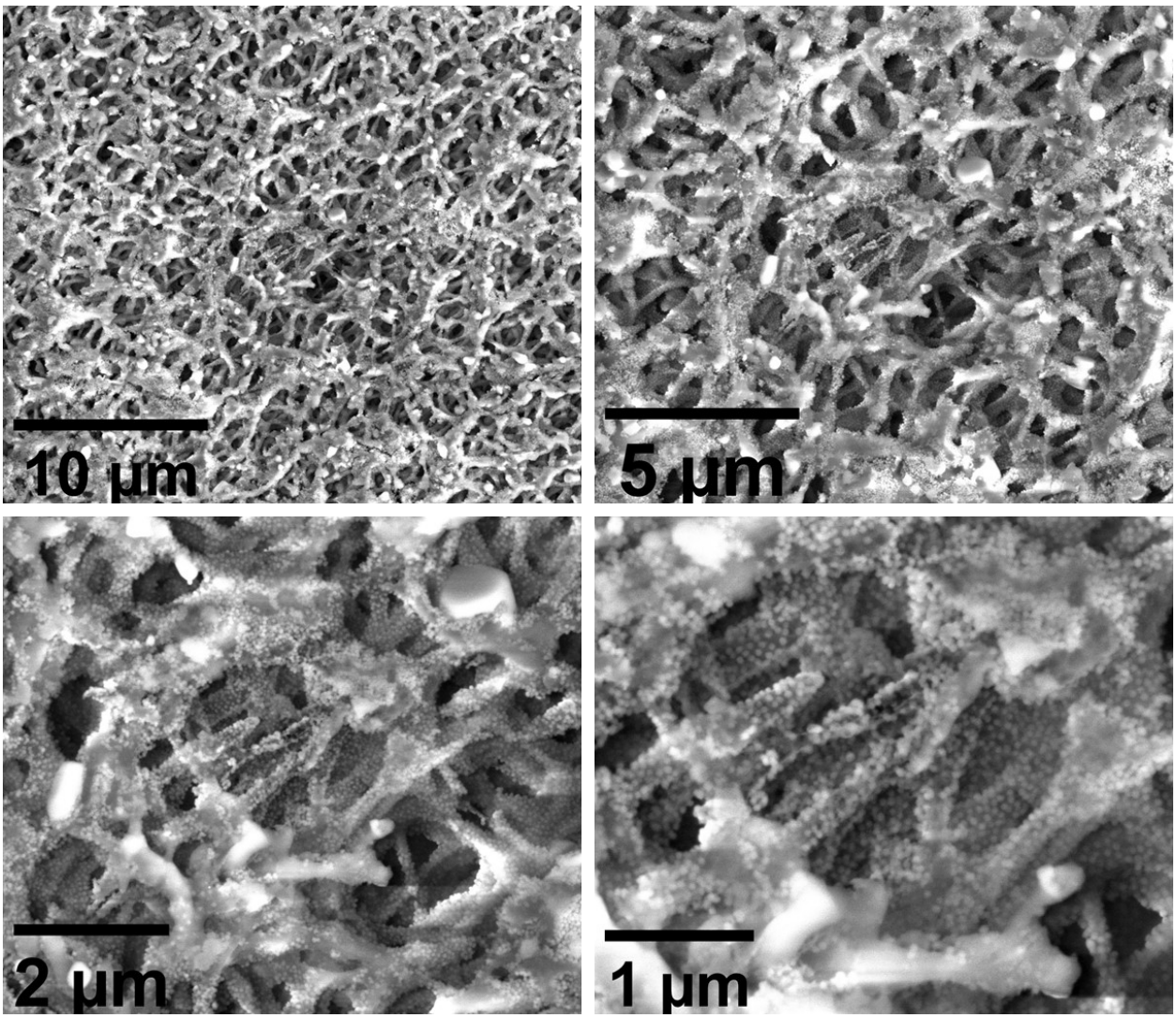

Figure S14. E-SEM images of inSNPs on native nanoporous regenerated cellulose (NRC).

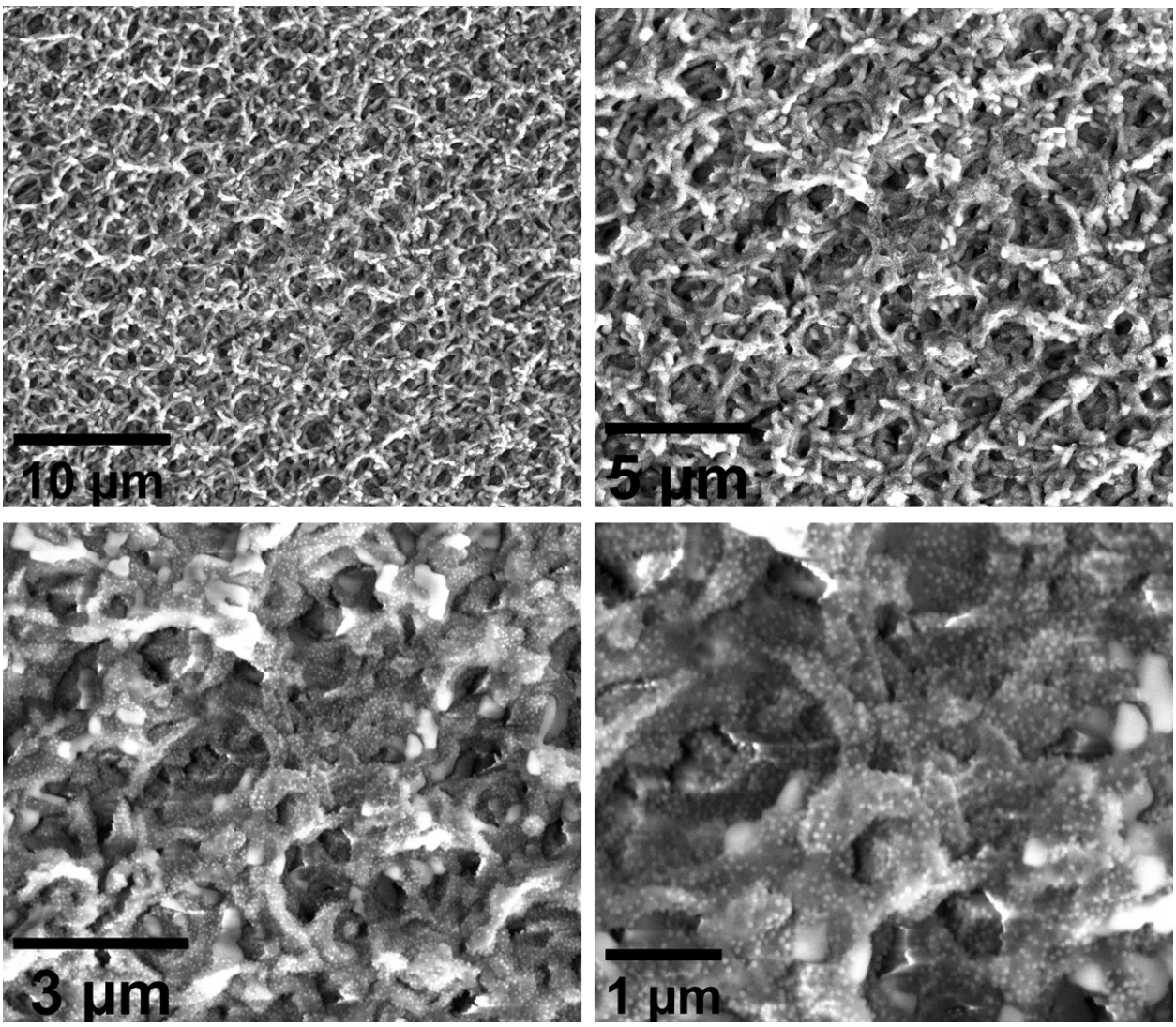

Figure S15. E-SEM images of inSNPs on PTA coated nanoporous regenerated cellulose (NRC).

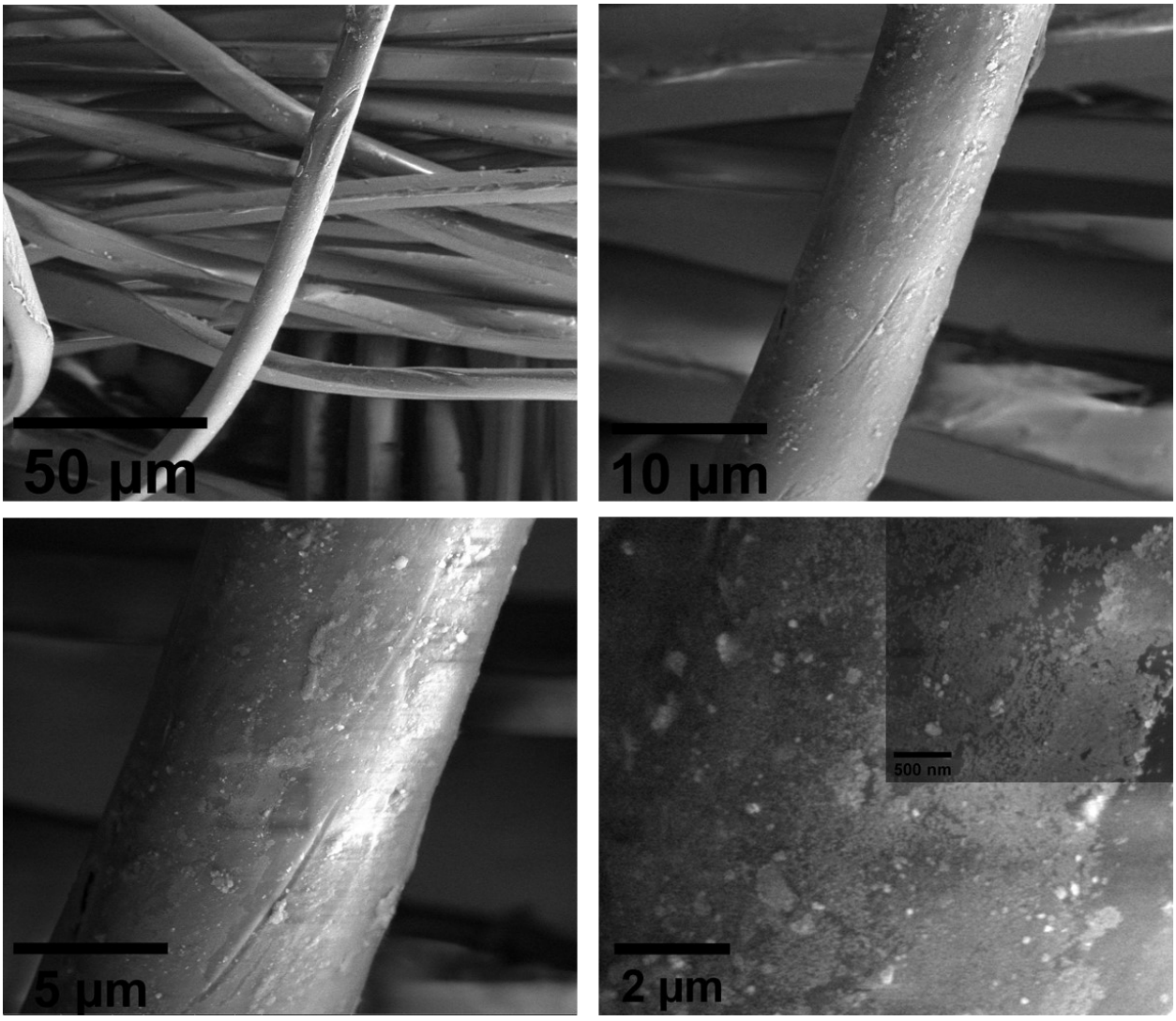

Figure S16. E-SEM images of inSNPs on native polyester fabric.

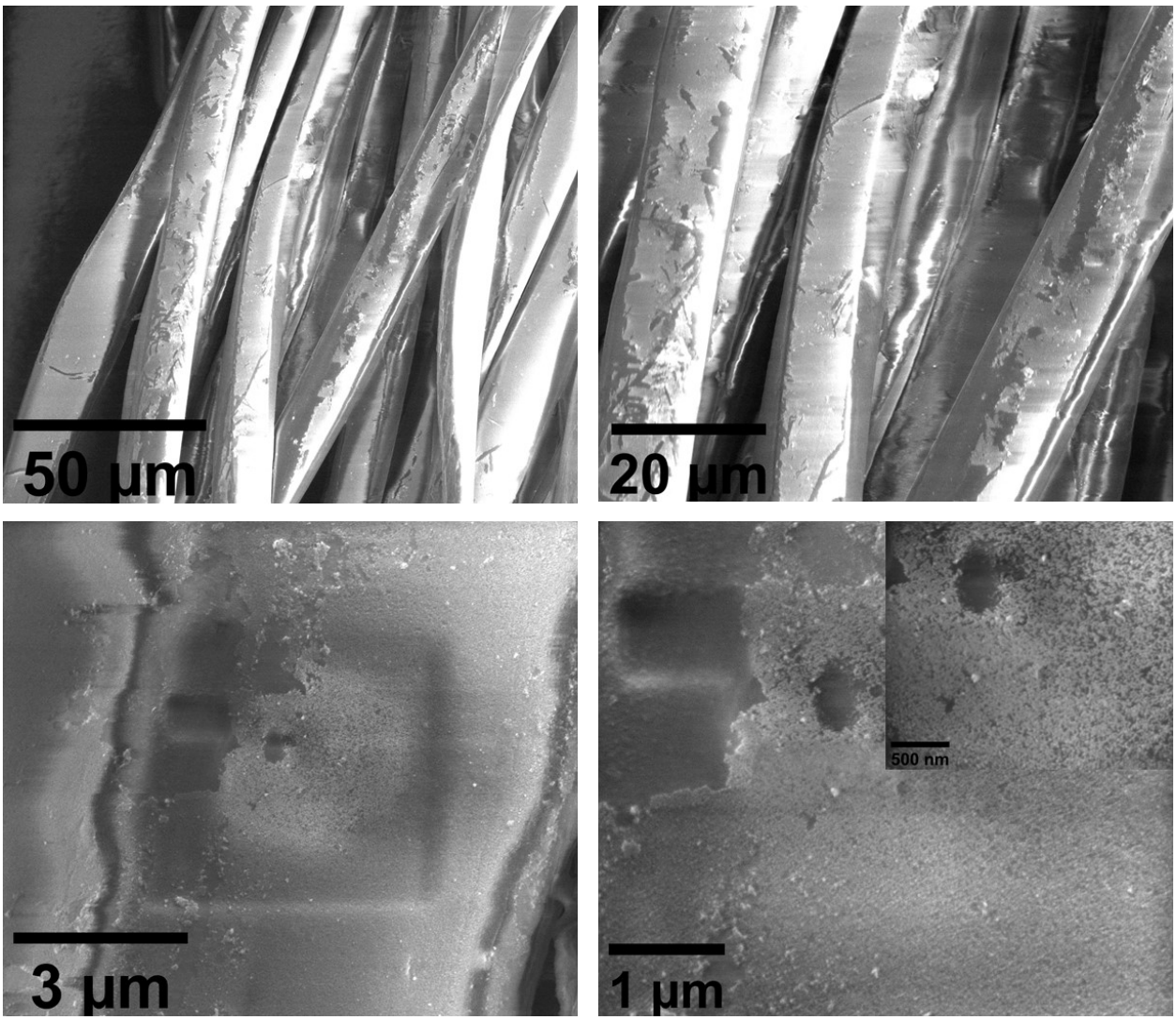

Figure S17. E-SEM images of inSNPs on PTA coated polyester fabric.

9. Analysis of E-SEM Images of inSNPs

Image analysis was applied to the E-SEM images of inSNP modified samples to measure the nanoparticle diameters and the surface coverage of the particles. Two widely used software programs—ImageJs[5] and CellProfiler[6] were used to crosscheck the particle diameter analysis. Figure S18 shows good agreement between the particle analysis results derived from the two techniques.

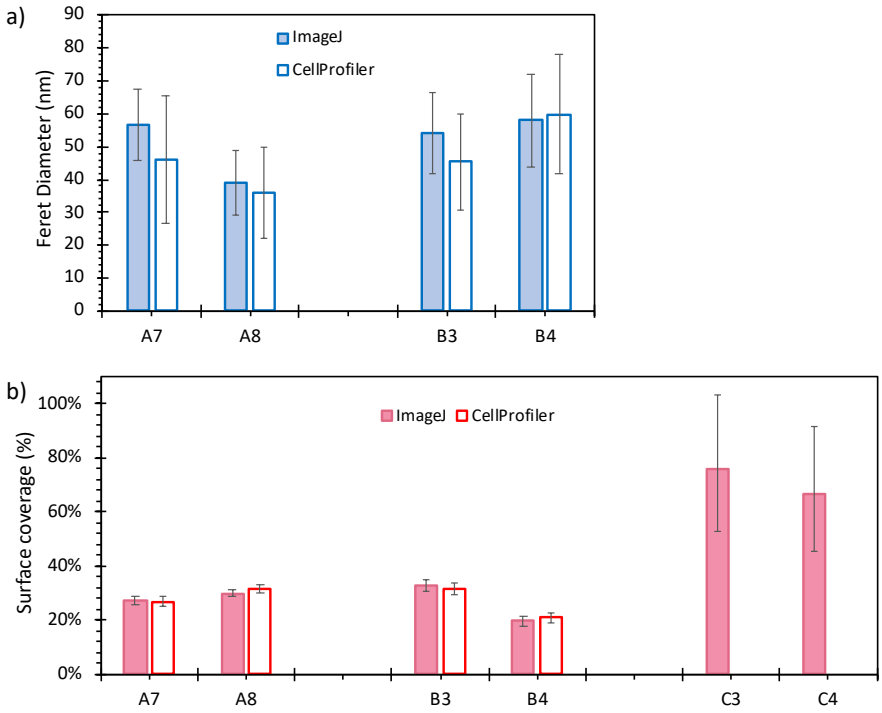

Figure S18. Comparison of image analysis results of inSNP E-SEM images obtained from ImageJ and CellProfiler. Panel (a) shows the inSNP diameters. Panel (b) shows the percentage surface coverage. The category labels refer to the panels shown in Figure 2 of the main text: A7 (native cotton), A8 (PTA-coated cotton), B3 (native NRC), B4 (PTA-coated NRC), C3 (native polyester), and C4 (PTA-coated polyester). Diameters for inSNP grown on polyester samples were not analyzed with software because the particles were too closely spaced together for consistent results to be obtained. Correspondingly, coverage on polyester was not obtained from CellProfiler because that analysis required particles to be identified. Error bars for diameters indicate ±1 SD of the particle size distribution. Error bars for surface coverage indicate the hypothetical changes if the thresholded areas were expanded or contracted by 1 pixel.

ImageJ particle analysis depended on image processing of E-SEM grayscale images to obtain a "thresholded" binary images of particle and non-particle areas. To allow more accurate thresholding, selected areas of the E-SEM images with fewer background features exhibiting differences in image "brightness" were cropped for analysis. These brightness variations are often produced by sample

charging and large changes in surface topography. An example of the imageJ analysis workflow (for inSNP grown on native cotton) is shown in Figure S19.

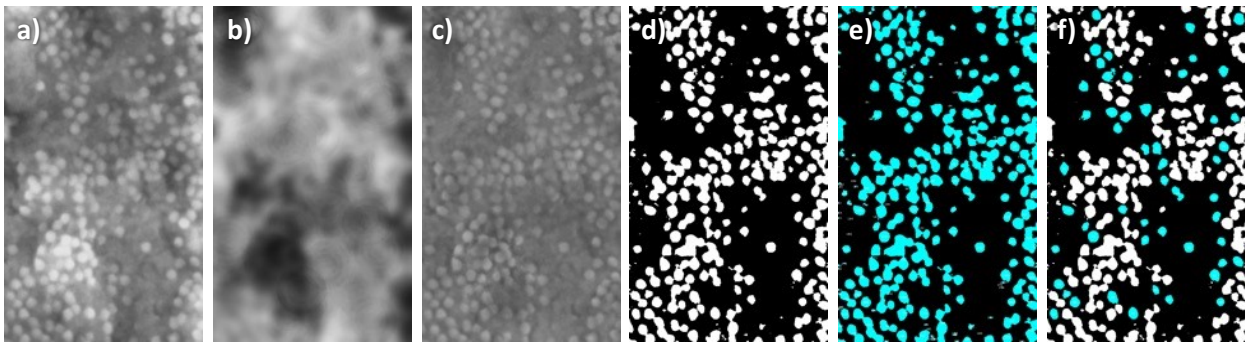

Figure S19. Series of images illustrating the ImageJ particle analysis work flow. The E-SEM image corresponding to inSNP modified native cotton sample is shown as an example. The original E-SEM grayscale image (a) was multiplied with a mask (b) obtained from Gaussian blurring of the original image. The result is an image with a "flat" background brightness (c) that can be more easily thresholded to show only areas with and without have particles (d). The particle areas were then automatically identified (in cyan) by the ImageJ particle analysis module (e). This allowed summing of the particle surface coverage. To obtain more accurate particle size measurements, the particle analysis was (re)applied with a circularity filter of < 1.5 to identify only those features that appeared as distinct isolated particles (f). The Feret diameter was used to match the output from CellProfiler (see Figure S20).

CellProfiler is a more advanced program and can better filter out background variations in "light" levels and also distinguish adjacent particles that appear joined in a thresholded image. Thus, in most cases the original uncropped E-SEM images could be used for analysis. Figure S20 shows the CellProfiler analysis results panel for the sample corresponding to the example shown in Figure S19. However, in the case of very small and closely packed inSNPs on polyester samples that were represented by few pixels each, it was difficult to set analysis parameters to both identify all particles and enable consistent particle size analysis. Thus CellProfiler was not used to calculate surface coverage for the inSNPs on polyester samples. At the same time, although ImageJ cannot distinguish "joined" particles, more accurate particle size results were obtained by including only single particles in the analysis (i.e. particles with circularity > 1.5 were excluded) and by the use of only image crops with fewer interfering features (see discussion above on background brightness). Overall, the ImageJ surface coverage results were more complete and the calculated particle size is a more accurate representation of the actual particles. Therefore, the ImageJ results were chosen for presentation in Table 1 of the main text. Nonetheless, the more automated analysis performed on wider fields of view using CellProfiler was able to corroborate the ImageJ results, as shown in Figure S18 by the closely matching results obtained by the two routines.

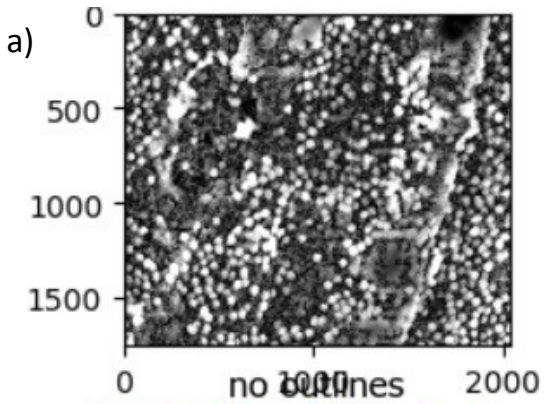

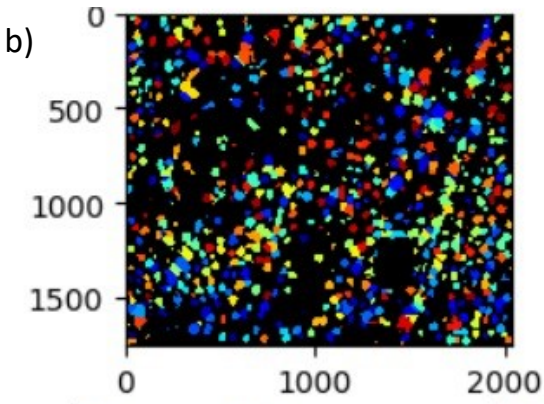

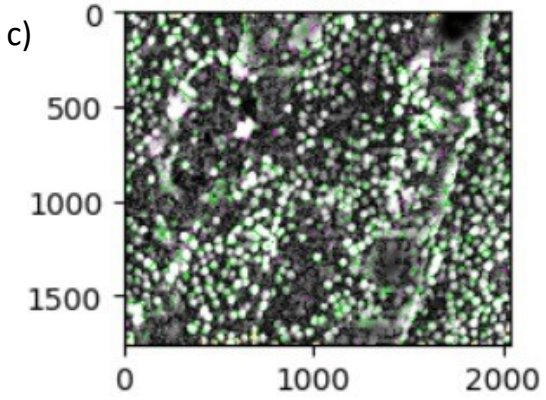

d)

# of accepted objects	876
10th pctile diameter	14.8 pixels
Median diameter	36.3 pixels
90th pctile diameter	51.6 pixels
Area covered by objects	26.8 %
Thresholding filter size	1.0
Threshold	0.459
Declumping smoothing filter size	6.7
Maxima suppression size	6.7

Figure S20. Example of CellProfiler image analysis results for the E-SEM image corresponding to the sample shown in Figure S17 (a inSNP modified native cotton sample). Most of the time, CellProfiler enabled the entire original E-SEM image (a) to be analyzed. The particle areas are identified and distinct individual particles are highlighted in different colors (b). The particles suitable for particle diameter calculations are shown in (c), and the results are tabulated in (d).

10. Enzyme Activity of IgG Immobilized on StöberSNPs vs. on inSNPs

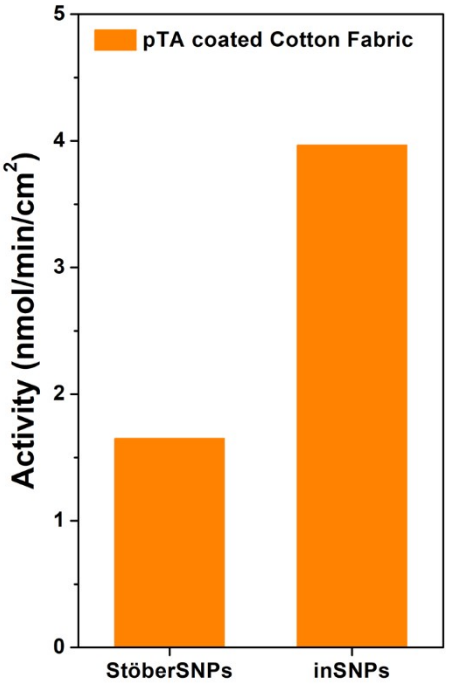

Figure S21. The activity (nmol/min/cm2) of 5µg/mL of IgG on StöberSNPs (20mg/mL) and inSNPs modified PTA coated cotton fabric (type II substrate) was measured after binding with anti-IgG-HRP. In-situ growth is more uniform and shows dense covering of the surface that results in ~2.4 times more activity than StöberSNPs on PTA coated cotton fabric.

11. Energy Dispersive X-Ray (EDX) Elemental Analysis

Our E-SEM (FEI Quanta 250) was also fitted with an EDX detector. As example, elemental analysis was performed on the same cotton samples as those imaged (see Figure 2 and Figures S7-17). During EDX measurements, an acceleration voltage of 10 kV was used. Typical EDX data of the cotton samples modified with silica NPs are shown below. As can be seen, although slicon (Si) peaks could be unambiguously discerned for both StöberSNP and inSNP samples, the relative Si and oxygen (O) peaks are much higher than for carbon (C) on inSNP samples. Since Si would have come solely from the silica NPs, C solely from the cellulose cotton substrate, and O from both silica and cotton, the dramatically increased levels of Si and O indicate much more numerous inSNP modification, corroborating the E-SEM images shown in Figure 2 and Figures S7-17

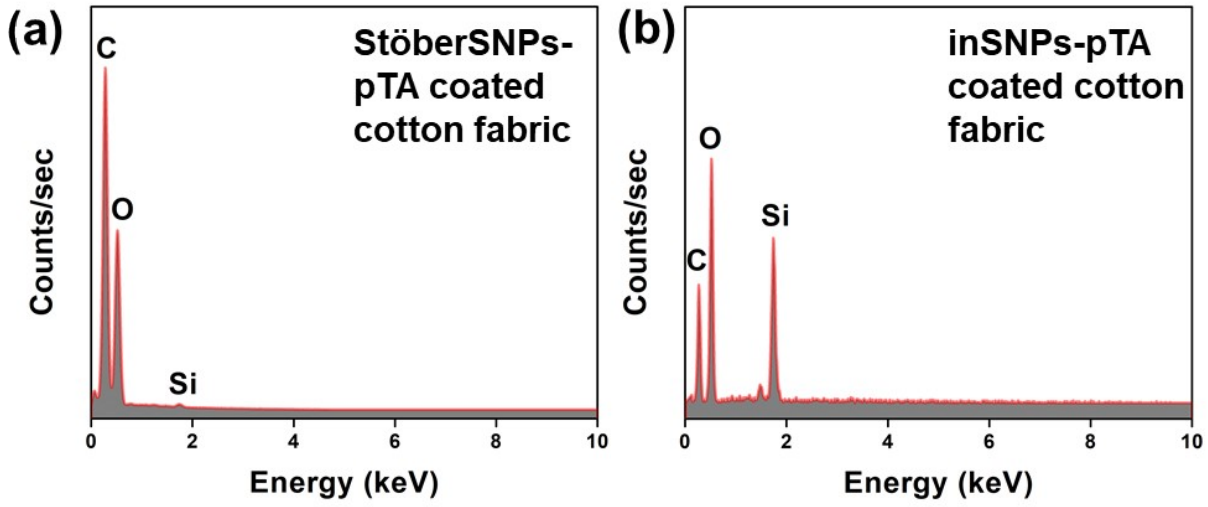

Figure S22. EDX spectrum of SNPs immobilized on PTA coated cotton fabric. (a) StöberSNPs (b) inSNPs.

12. Nanostructured Based Surface Area Enhancement

The native "flat" surface on the fibers limits the amount of functional molecules that can be immobilized. Nanoparticle (NP) modification of attachment to the surface provides a potentially convenient method of increasing surface area without compromising the substrate structure as it transforms a two-dimensional (2-D) surface into a three-dimension (3-D) one with additional surfaces protruding from the substrate. Assuming that our inSNPs nucleate and grow isotropically from the fiber surface, hemispherical NPs would be added to the surface. Each of such idealized inSNPs increases the area of a surface by half the area of a sphere ($4\pi r^2/2 = 2\pi r^2$; Figure S23). However, each such inSNP also covers an area of the fiber equal to its circular footprint, which is πr^2 (Figure S23). In other words, for each inSNP, an area of the fiber surface equal to πr^2 is replaced by a hemispherical protrusion of area $2\pi r^2$, i.e., the surface area is doubled wherever there is inSNP coverage.[7] Thus in Table 1 in the main text, the surface area increase is shown as double the coverage of inSNPs.

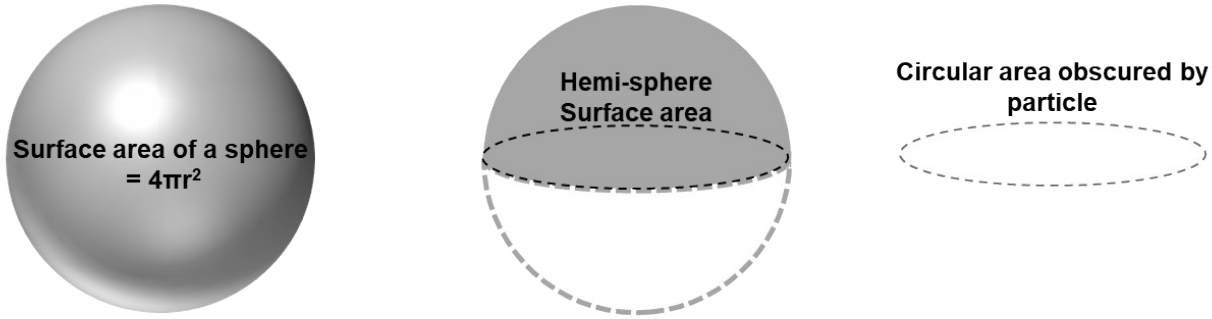

$$Area\ of\ a\ circle = A = \pi r^2$$

$$\begin{aligned} The\ curved\ surface \text{ area of a hemisphere} &= \text{half of the surface area of a sphere} \\ &= \frac{1}{2} * 4\pi r^2 \\ &= 2\pi r^2 \end{aligned}$$

$$Area\ of\ a\ hemisphere\ is\ double\ the\ area\ of\ a\ flat\ circle$$

Figure S23. Comparison between the surface areas of a sphere, a hemisphere, and a circular footprint.

Note that this is hemispherical estimation is a lower-bound of the surface area increase. From E-SEM images (Figure 2 and Figures S7-17), some inSNPs appear to protrude further away from the surface and have a slight undercut (they might have grown from nanometer sized seeds already nucleated in solution). However, because the IgG and SA protein themselves have a significant size (6 to 14 nm, see main text), the restricted space around any undercut would not fit any proteins. Hence, there is likely little significant increase in terms of "usable" area for protein immobilization.

13. Estimation of Sample Fiber Surface Areas

Table S6. Specific fiber surface areas of cotton, PE and NRC samples.

	Cotton[a]	Polyester (PE) [a]	NRC[b]
Polymer density	1.52 g/cm^3	1.38 g/cm^3	1.52 g/cm^3
Fiber diameter	15 μm	15 μm	0.2 μm
Fabric weight	108 g/m^2	61.3 g/m^2	27.4 g/m^2
Estimated specific surface area	0.18 m^2/g	0.19 m^2/g	2.96 m^2/g
Estimated total fiber surface area	19 cm^2 (per 1x1 cm^2 sample)	12 cm^2 (per 1x1 cm^2 sample)	107 cm^2 (per 1x1 cm^2 sample)

[a]*BET measurement;* [b]*microscopy based estimation (Figure 2 and Figures S7-17).*

Since our samples are composed of fibers, they are porous substrates. Their outward, apparent sizes are standardized to 1x1 cm^2 but they have internal surface areas many times higher. The specific surface areas of our cotton, PE and NRC samples are listed in Table S6. The NRC data is taken from our previous study,[1] measured by Brunauer–Emmett–Teller (BET) isotherm analysis of nitrogen adsorption measurements (on a Micromeritics ASAP 2020). Cotton and PE specific areas were estimated from how many fibers of an average diameter characterized in microscopy images is required to match the measured weight per area of the fabric. An example calculation is given below.

The density of cellulose is ca. 1.52 g/cm^3. The density of the woven cotton fabric is measured to be 0.0108 g/cm^2. The cellulosic material therefore occupies a volume equivalent to a fully dense layer of material of thickness = $\frac{0.0108\ g/cm^2}{1.52\ g/cm^3}$ = 0.00709 cm (71 μm). The cross-sectional area per 1 cm^2 of such a layer of fabric is 71 μm x 1 cm = 7.1 x10^{-7} m^2. SEM characterization shows that each fiber is ca. 10 – 15 μm in diameter, thus having a cross sectional area (πr^2) each of 177 μm^2 = 1.77 x 10^{-10} m^2 (value range corresponds to the range in estimated fiber diameters). Thus, the number of fibers needed to fill the cross-sectional area, assuming for the sake of calculation that each fiber stretches spans the 1 cm wide sample $= \frac{fabric\ cross-section}{fiber\ cross-section} = \frac{7.1\ x\ 10^{-7} m^2}{1.77\ x\ 10^{-10} m^2}$ = 4.0 x 10^3. At the same time, the surface area of each of these hypothetical fibers = circumference x length = 2□r x 1 cm = 4.71 x 10^{-7} m^2. For the number of hypothetical fibers present, the fiber surface area available per 1 cm^2 of the woven cotton would be 4.0

x 10^3 x 4.71 x 10^{-7} m^2 = 19 cm^2. Given the weighed density of the woven cotton, the equivalent specific surface area = $\frac{19\ cm^2/cm^2}{0.0108\ g/cm^2}$ = 0.18 m^2/g.

14. Activity Comparison on Cotton, NRC and PE

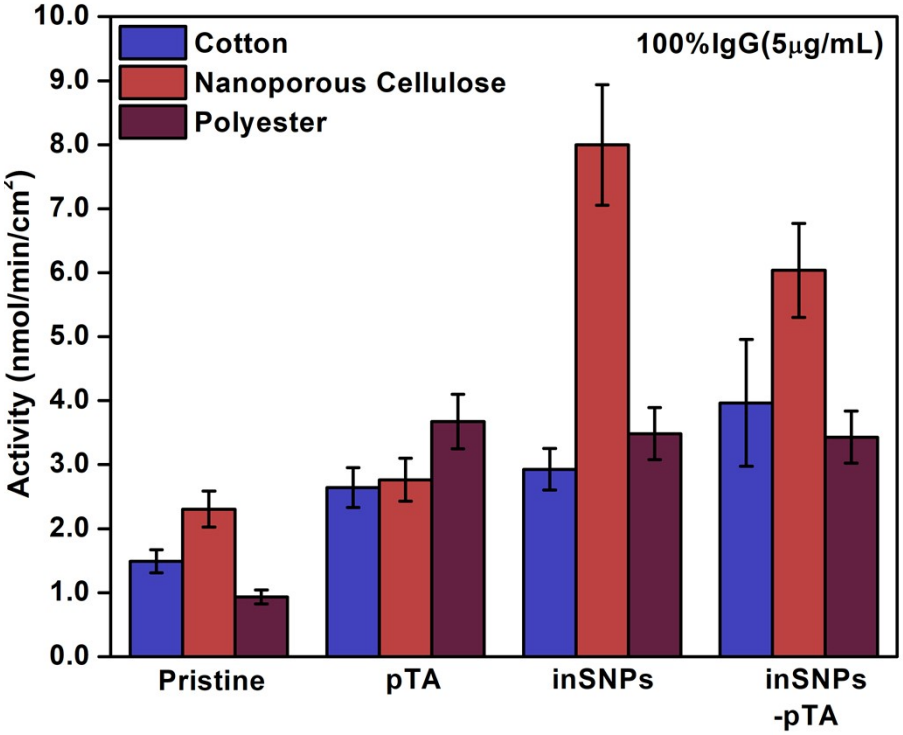

Figure S24. Native/Pristine and functionalized cotton, NRC, and polyester samples type I-IV immobilized with 5μg/mL IgG. These results indicate that native polyester displayed significantly lower activity than native cotton even though both our fabrics have similar intrinsic fiber surface areas, whereas the relatively similar cellulosic chemistries of NRC and cotton but the 7-times higher intrinsic fiber surface area on NRC.

15. Second PTA Coating on inSNP Modified PTA-Cotton

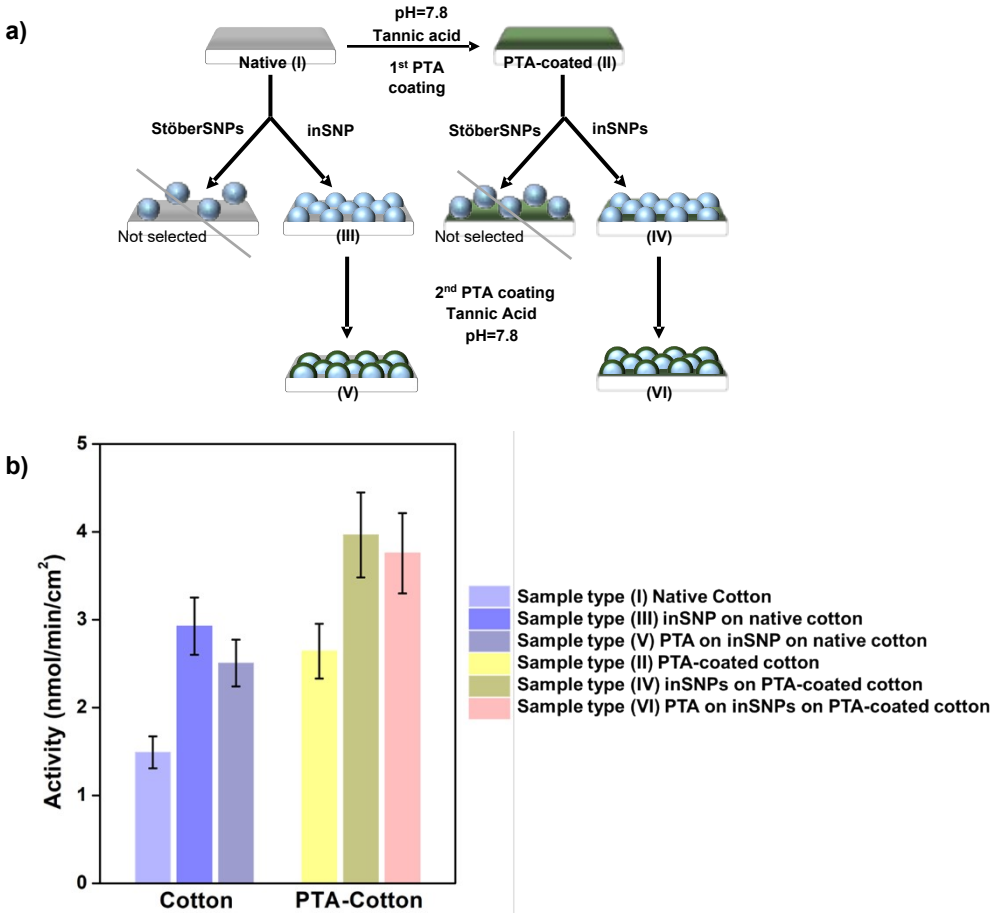

Figure S25. a) Schematic of functionalization steps. In addition to the sample types I-IV shown in Figure 1a of the main text, a "second" PTA coating was applied to generate sample types V and VI that, respectively, had and did not have a first PTA coating prior to inSNP modification. b) Comparison of immobilized IgG surface activities with different combinations of PTA coatings and inSNP modifications on cotton samples, including a second PTA coating on inSNP modified with a first PTA coating on cotton. PBS solutions with 5 µg.mL-1 IgG alone was used.

16. Effect of Increasing IgG Concentration

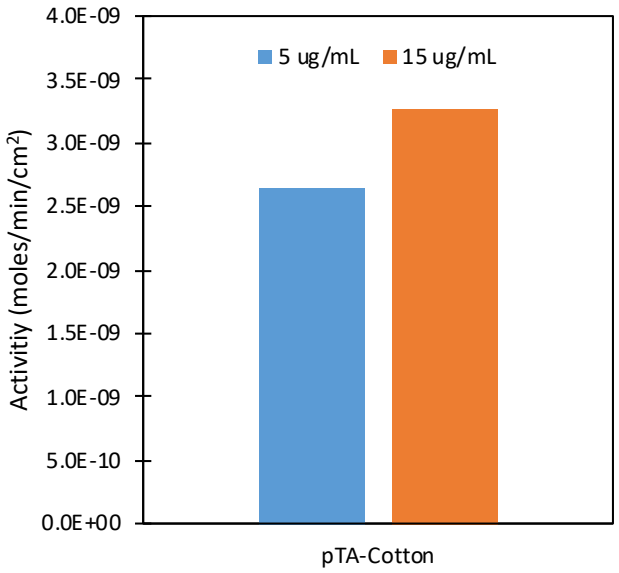

Figure S26. Comparison of immobilized IgG surface activities on PTA-coated cotton using solutions containing 5 µg.mL-1 and 15 µg.mL-1 IgG.

17. Activities After 7 Days' Storage

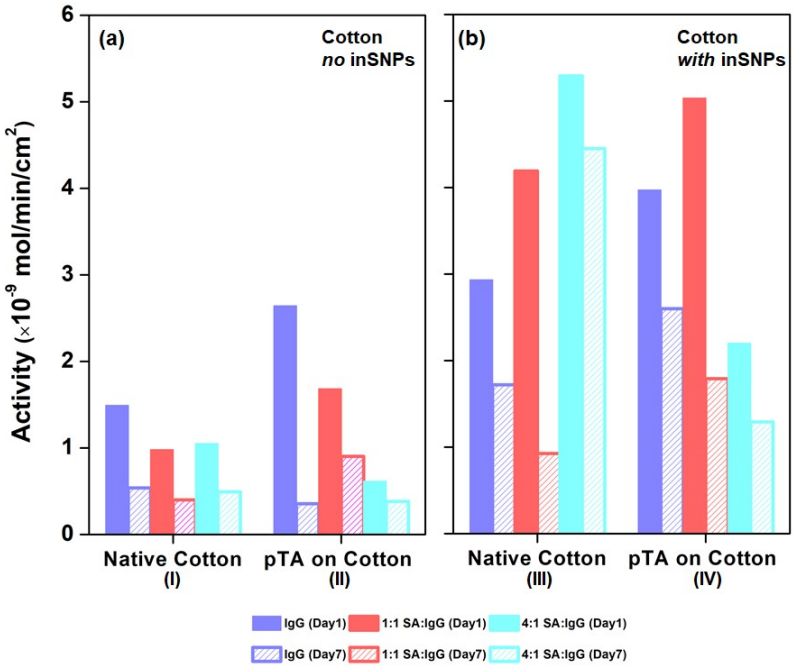

Figure S27. Comparison of activities from bound anti-IgG-HRP measured on cotton with and without inSNP before and after seven days' storage at 4°C. The Roman numerals on the x-axis refer to the substrate preparation procedure shown in Figure 1**.**

18. Tables of Surface Activity Values

Table S7. Raw activity values measured for IgG and BSA immobilized on cotton fabric. The sample type labels refer to Figure S25.

Sr. No.	Material	Activity (nmol/min/cm^2) IgG and BSA ratios				
		100% IgG (5µg/mL)	**1:1 (IgG:BSA) (5:5µg/mL)**	**1:2 (IgG:BSA) (5:10µg/mL)**	**1:4 (IgG:BSA) (5:20µg/mL)**	**1:9 (IgG:BSA) (5:45µg/mL)**
1.	Cotton (I)	1.5 ± 0.2	1 ± 0.1	1 ± 0.1	1.1 ± 0.1	1.5 ± 0.2
2.	PTA coated Cotton (II)	2.6 ± 0.3	1.7 ± 0.1	0.8 ± 0.1	0.6 ± 0.1	1.2 ± 0.1
3.	inSNPs Cotton (III)	2.9 ± 0.3	4.2 ± 0.5	3.8 ± 0.5	5.3 ± 0.7	0.7 ± 0.1
4.	inSNPs on PTA coated Cotton (IV)	4 ± 0.5	5 ± 0.6	3 ± 0.4	2.2 ± 0.3	1.2 ± 0.1
5.	PTA coated inSNPs Cotton (V)	2.5 ± 0.3	3 ± 0.3	2.6 ± 0.2	1.4 ± 0.1	0.8 ± 0.1
6.	PTA coated inSNPs on	3.8 ± 0.5	2.7 ± 0.3	2.8 ± 0.3	1.4 ± 0.2	0.7 ± 0.1

	PTA coated Cotton (VI)					

Table S8. Normalized activity values measured for IgG and BSA immobilized on cotton fabric. The sample type labels refer to Figure S25.

Sr. No.	Material	Normalized Activity IgG and BSA ratios				
		100% IgG (5µg/mL)	**1:1 (IgG:BSA) (5:5µg/mL)**	**1:2 (IgG:BSA) (5:10µg/mL)**	**1:4 (IgG:BSA) (5:20µg/mL)**	**1:9 (IgG:BSA) (5:45µg/mL)**
1.	Cotton (I)	1	0.67	0.66	0.71	1.01
2.	PTA coated Cotton (II)	1.77	1.19	0.55	0.41	0.12
3.	inSNPs Cotton (III)	1.96	2.81	2.52	3.55	0.49
4.	inSNPs on PTA coated Cotton (IV)	2.66	3.37	2.04	1.47	0.8
5.	PTA coated inSNPs Cotton (V)	1.68	2.02	1.75	0.94	0.52
6.	PTA coated inSNPs on PTA coated	2.52	1.81	1.88	0.95	0.49

	Cotton (VI)					

Table S9. The mass density (ng/cm^2) of immobilized IgG estimated from the amount of HRP bound that corresponds to the activities shown in Table S7 and scaled by the fiber surface area shown in Table S6. The sample type labels refer to Figure S25. The calculation assumes that each anti-IgG-HRP binds to one immobilized IgG, which corresponds to the fact that the anti-IgG-HRP is the anti-mouse antibody raised against the immobilized mouse IgG. The mass density of HRP bound was first calculated from the activities measured (Table S7) and the calibration of activity against HRP mass shown in Figure S6. HRP is a 44 kDa protein while IgG is a ca. 150 kDa protein. Therefore, mass of HRP obtained was multiplied by 3.4-times (150 kDa/44 kDa) to obtain the corresponding immobilized IgG mass density on each 1x1 cm^2 sample.

Sr. No.	**Material**	**Mass Density (ng/cm^2) of Immobilized IgG**				
		100% IgG (5µg/mL)	**1:1 (IgG:BSA) (5:5µg/mL)**	**1:2 (IgG:BSA) (5:10µg/mL)**	**1:4 (IgG:BSA) (5:20µg/mL)**	**1:9 (IgG:BSA) (5:45µg/mL)**
1.	Cotton (I)	170 ± 0.2	111 ± 0.1	117 ± 0.1	120 ± 0.1	172 ± 0.2
2.	PTA coated Cotton (II)	301 ± 0.3	191 ± 0.2	93 ± 0.1	70 ± 0.1	132 ± 0.1
3.	inSNPs Cotton (III)	333 ± 0.3	477 ± 0.5	428 ± 0.5	602 ± 0.7	83 ± 0.1
4.	inSNPs on PTA coated Cotton (IV)	451 ± 0.5	572 ± 0.7	346 ± 0.4	250 ± 0.3	136 ± 0.1
5.	PTA coated	285 ± 0.3	343 ± 0.3	296 ± 0.2	160 ± 0.1	88 ± 0.1

	inSNPs Cotton (V)					
6.	PTA coated inSNPs on PTA coated Cotton (VI)	428 ± 0.5	306 ± 0.4	318 ± 0.3	160 ± 0.2	83 ± 0.1

Table S10. Raw and normalized activity values measured for IgG and BSA immobilized on NRC.

Sr. No.	**Material**	**Activity (nmol/min/cm^2) IgG and BSA ratios**		
		100% IgG (5µg/mL)	**1:1 (IgG:BSA) (5:5µg/mL)**	**1:4 (IgG:BSA) (5:20µg/mL)**
1.	NRC (I)	2.3 ± 0.3	0.6 ± 0.1	0.2 ± 0.02
2.	PTA coated NRC (II)	2.8 ± 0.3	0.7 ± 0.1	1.4 ± 0.2
3.	inSNPs NRC (III)	8 ± 0.9	6.4 ± 0.7	7.2 ± 0.9
4.	inSNPs on PTA coated NRC (IV)	6 ± 0.7	5.1 ± 0.6	4.1 ± 0.5
Sr. No.	**Material**	**Normalized Activity**		
		100% IgG (5µg/mL)	**1:1 (IgG:BSA) (5:5µg/mL)**	**1:4 (IgG:BSA) (5:20µg/mL)**
1.	NRC (I)	1	0.2	0.1
2.	PTA coated NRC (II)	1.2	0.3	0.6
3.	inSNPs NRC (III)	3.5	2.8	3.1

4.	inSNPs on PTA coated NRC (IV)	2.6	2.2	1.8

Table S11. Raw and normalized activity values measured for IgG and BSA immobilized on polyester.

Sr. No.	**Material**	**Activity (nmol/min/cm^2) IgG and BSA ratios**		
		100% IgG (5µg/mL)	**1:1 (IgG:BSA) (5:5µg/mL)**	**1:4 (IgG:BSA) (5:20µg/mL)**
1.	Polyester (I)	0.9 ± 0.1	0.9 ± 0.1	1.3 ± 0.1
2.	PTA coated Polyester (II)	3.7 ± 0.4	2.7 ± 0.3	3.9 ± 0.4
3.	inSNPs Polyester (III)	3.5 ± 0.4	2.9 ± 0.3	2.9 ± 0.4
4.	inSNPs on PTA coated Polyester (IV)	3.4 ± 0.4	2.7 ± 0.3	4 ± 0.5
Sr. No.	**Material**	**Normalized Activity**		
		100% IgG (5µg/mL)	**1:1 (IgG:BSA) (5:5µg/mL)**	**1:4 (IgG:BSA) (5:20µg/mL)**
1.	Polyester (I)	1	1	1.4
2.	PTA coated Polyester (II)	3.9	2.9	4.2
3.	inSNPs Polyester (III)	3.7	3.1	3.1

4.	inSNPs on PTA coated Polyester (IV)	3.7	2.9	4.2

19. Tables of P values shown in Figure 3 and 4

Table S12. The Student t-test was applied to calculate p-values for Native and pTA coated fibers with and without inSNP and with 100% IgG immobilized.

Figure 3b - Native fibers	
	Cotton *with* inSNPs
Cotton *no* inSNPs	0.0238
	NRC *with* inSNPs
NRC *no* inSNPs	0.0030
	Polyester *with* inSNPs
Polyester (PE) *no* inSNPs	0.0009
Figure 3c - PTA on fibers	
	PTA Cotton *with* inSNPs
PTA Cotton *no* inSNPs	0.0618
	PTA NRC *with* inSNPs
PTA NRC *no* inSNPs	0.0267
	PTA Polyester (PE) *with* inSNPs
PTA Polyester *no* inSNPs	0.6220

Table S13. The Student t-test was applied to calculate p-values for each sample type w.r.t sample immobilized with 100% IgG.

Figure panel and sample types	**1:1 SA:IgG**	**2:1 SA:IgG**	**4:1 SA:IgG**	**9:1 SA:IgG**
(a) Cotton with inSNPs				
Native Cotton	0.1427	0.1559	0.0713	0.0005
PTA on Cotton	0.4327	0.2925	0.0481	0.0009
(d) Cotton *no* inSNPs				
Native Cotton	0.2745	0.0990	0.1354	0.8135
PTA on Cotton	0.1031	0.0029	0.0020	0.0381
(b) NRC with inSNPs				
Native NRC	0.3195	-	0.8865	-
PTA NRC	0.2451	-	0.1757	-
(e) NRC *no* inSNPs				
Native NRC	0.0013	-	0.0001	-
PTA NRC	0.0011	-	0.0243	-
(c) Polyester (PE) with inSNPs				
Native PE	0.5334	-	0.6445	-
PTA on PE	0.5642	-	0.4209	-
(f) Polyester (PE) *no* inSNPs				
Native PE	0.7693	-	0.2544	-
PTA on PE	0.2988	-	0.9373	-

20. References

1. A. M. Sousa, T.-D. Li, S. Varghese, P. J. Halling and K. H. Aaron Lau, *ACS Appl. Mater. Interfaces*, 2018, **10**, 39353-39362.
2. W. Stöber, A. Fink and E. Bohn, *J. Colloid Interface Sci.*, 1968, **26**, 62-69.
3. D. C. Manatunga, R. M. de Silva and K. N. de Silva, *J Applied Surface Science*, 2016, **360**, 777-788.
4. P. J. Cumpson and M. P. Seah, *Surface and Interface Analysis: An International Journal devoted to the development and application of techniques for the analysis of surfaces, interfaces and thin films*, 1997, **25**, 430-446.
5. C. A. Schneider, W. S. Rasband and K. W. J. N. m. Eliceiri, 2012, **9**, 671-675.
6. C. McQuin, A. Goodman, V. Chernyshev, L. Kamentsky, B. A. Cimini, K. W. Karhohs, M. Doan, L. Ding, S. M. Rafelski and D. J. P. b. Thirstrup, 2018, **16**, e2005970.
7. K. Woeppel, X. Zheng and X. J. J. o. M. C. B. Cui, 2018, **6**, 3058-3067.